



**HAL**  
open science

# Stark Effect of Interactive Electron-hole pairs in Spherical Semiconductor Quantum Dots

Baptiste Billaud, Marco Picco, Tuong T. Truong

► **To cite this version:**

Baptiste Billaud, Marco Picco, Tuong T. Truong. Stark Effect of Interactive Electron-hole pairs in Spherical Semiconductor Quantum Dots. 2009. hal-00385434v1

**HAL Id: hal-00385434**

**<https://hal.science/hal-00385434v1>**

Preprint submitted on 19 May 2009 (v1), last revised 14 Aug 2009 (v3)

**HAL** is a multi-disciplinary open access archive for the deposit and dissemination of scientific research documents, whether they are published or not. The documents may come from teaching and research institutions in France or abroad, or from public or private research centers.

L'archive ouverte pluridisciplinaire **HAL**, est destinée au dépôt et à la diffusion de documents scientifiques de niveau recherche, publiés ou non, émanant des établissements d'enseignement et de recherche français ou étrangers, des laboratoires publics ou privés.

# Stark Effect of Interactive Electron-hole pairs in Spherical Semiconductor Quantum Dots

B. Billaud<sup>1,2</sup>‡, M. Picco<sup>1</sup>, and T.-T. Truong<sup>2</sup>

E-mail: [bbillaud@u-cergy.fr](mailto:bbillaud@u-cergy.fr)

<sup>1</sup>Laboratoire de Physique Théorique et Hautes Energies (LPTHE),  
CNRS UMR 7589, Université Pierre et Marie Curie (Paris VI),  
4, place Jussieu, 75252 Paris Cedex 05, France.

<sup>2</sup>Laboratoire de Physique Théorique et Modélisation (LPTM),  
CNRS UMR 8089, Université de Cergy-Pontoise,  
2, avenue Adolphe Chauvin, 95302 Cergy-Pontoise Cedex, France.

**Abstract.** We present a theoretical variational approach, based on the effective mass approximation (EMA), to study the quantum-confinement Stark effects for spherical semiconducting quantum dots in the strong confinement regime of interactive electron-hole pair and limiting weak electric field. The respective roles of the Coulomb potential and the polarization energy are investigated in details. Under reasonable physical assumptions, analytical calculations can be performed. They clearly indicate that the Stark shift is a quadratic function of the electric field amplitude in the regime of study. The resulting numerical values are found to be in good agreement with experimental data over a significant domain of validity.

PACS numbers: 71.35.-y, 71.70.Ej

Submitted to: *Journal of Physics: Condensed Matter*

‡ To whom correspondence should be addressed.

## 1. Introduction

Depending on their dimensionality, nano-structures displaying many effects of standard atomic physics are known as quantum dots, quantum wires or quantum wells. For about two decades, they are produced by diverse techniques such as etching, local inter-diffusion, particle suspension in dielectric media, or by self-assembly in matrices of a host material and are known as confined systems. In these structures, the motion of one to a hundred embedded elementary charge carriers, which may be conduction band electrons, valence band holes, or excitons of the semiconducting host substrate, is restricted to a confined space region. In particular, since two Quantum Dots (QDs) are never identical in contrast to atoms, because of the crucial role of phonons or surface and bulk disorder on their electronic properties, a QD may be considered as a giant artificial atom, which enjoys prospects for an increasing range of future applications: *e.g.* as a semiconductor laser [1] or as single [2], as *qubits* for quantum information processing [3], as single-electron transistors in micro-electronics [4], as artificial *fluorophores* for intra-operative detection of tumors, biological imaging or cell studies, *etc.* [5]. In short, a QD presents the invaluable property of a device with an adjustable quantized energy spectrum, controlled by its size.

Thanks to the progress of semiconductor growth technology during the early eighties, quantum size effects (QSE) experimentally showed up in spherical semiconductors QDs, through optical properties of semiconductor micro-crystals embedded in an insulating matrix [6, 7]. The characteristic blue-shift observed in optical spectra of such strongly quantum-confined systems emerges in a widening of semiconductor optical band gap, due to the increasing confinement energy for decreasing QD size [8]. This fact has been observed in a large range of other confined micro-structures, *e.g.* in quantum ribbons or quantum disks [9], in quantum wires [10], indeed also in quantum wells [11]. The first theoretical attempt to describe electronic properties of semiconductor QDs has been elaborated upon a *particle-in-a-sphere* model in the effective-mass approximation (EMA), which assumes parabolic valence and conduction bands [8, 12–15]. Both electron and hole behave as free particles but trapped in a spherical infinite potential well and moving with different effective masses, commonly defined through the inverse of the second derivative of their kinetic energy with respect to their momentum, as a consequence of the parabolic energy bands assumption. The electron-hole Coulomb interaction is usually included and the excitonic contribution to the ground state energy is taken into account by Ritz' variational principle. Some other authors have developed their own EMA-model based on finite potential wells and have improved agreement with experimental data for a significant range of QD size [15–20]. In addition to spherical clusters, the case of cylindrical shaped micro-crystallites has been carefully treated and experimentally studied [16, 21–23], as well as the case of quantum wires [24, 25]. Of course, more sophisticated models, which consider non-parabolic valence and/or conduction band(s) have been also considered [26–30].

Among many important topics, it is the physics of atom-like behavior of QDs,

which is nowadays most vigorously investigated experimentally and theoretically in a large range of quantum confined systems, for potential technological applications. Of particular interest is the interaction with an ambient electromagnetic field, giving rise to the so-called quantum-confinement Stark effects (QCSE), which consists of an observable red-shift of the optical transition induced by the presence of a constant external electric field [31–34]. Moreover, in recent years, some works have emerged dealing with ac-electric field [35,36]. Stark effect leads to an energy shift of the exciton photoluminescence as well as a corresponding enhancement of its recombination lifetime [37]. The electric field dependence of QCSE was first studied in *GaAs* – *AlGaAs* multi-layers quantum wells [38]. Exciton energy shift peaks were experimentally observed and successfully compared to theoretical results obtained by a perturbation method introduced in [39], for the case of an applied electric field perpendicular to the plane of the layer wells, in which the Coulomb potential describing the electron-pair dynamics is not accounted for. In higher dimensional confinement, the Coulomb potential turns out to be more significant in QDs with spherical shape, and should not be neglected [40,41]. Finally, we observe that, over the years, the spherical structure has remained a very popular research domain to study theoretically and/or empirically QCSE [42–46].

In spite of an impressive number of published works, to the best of our knowledge, no simple comprehensive model, which describes Stark effects in spherical QDs with analytic results seems to be worked out. In this paper, we propose to use the EMA-model for spherical semiconductor micro-crystals, in order to establish analytically some criterions on the QD radius and on the electric field amplitude, and to understand why presently known results fail so far to correctly describe QCSE for a wide range of QD radius. To this end, we shall introduce in Section 2 our model first without electric field and recall some of its general properties. The next two Sections 3 and 4 are devoted to the analysis of Stark effects in spherical semiconductor nano-structures, first with the inclusion of electron-hole Coulomb potential and second with an additional polarization energy. In the concluding section, we summarize our main results and indicate possible future research perspectives.

## 2. EMA Quantum Dot model

In order to describe spherical semiconductor nano-structures interacting with a fixed external electric field, we study first a standard EMA-model with infinite spherical confining potential well, without electron-hole spin coupling and without spin coupling to applied external magnetic field. We shall see how such a model would allow us to perform analytically most of the calculations. There exists other models with parabolic confinement [47,48] or parabolic potential superimposed to an infinite potential well [49], which are used to explain certain spectroscopic data, but then the concept of a QD size is not so well defined.

As Stark effect in semiconducting micro-crystallites manifests itself through an energy shift of the electron-hole total energy levels due to the electric field presence,

we have to deal mainly with energy eigenvalue differences of a Hamiltonian. The most important idea, we must keep in mind, is that two different energies have to be computed in the same theoretical QD model. Even if this model does not fully describe the QD behavior in the absence of electric field, particularly for small QD radii, it can be still used and gives rather satisfactory theoretical predictions for Stark effects. The possible over- or under-estimation made for the electric field free electron-hole pair energy levels should also appear in the interaction of the electric field with electron-hole pairs. Then, it should be subtracted off from each other in order to get an approximated value for the Stark shift. Despite the fact that such an approach presents some intrinsic basic limitations, we shall adopt it, under some consistency conditions, to compute QCSE in semiconductor QDs.

### 2.1. Consistency conditions

Since most synthesized nano-crystallites possess an *aspect ratio* (defined as the ratio between the longest and shortest axes of the QD) smaller than 1.1, even if there exist also some experimental protocols, which lead to higher aspect ratio in micro-crystals, the hypothesis of a QD with spherical symmetry seems often to be quite reasonable.

Next, the effective potential at the QD surface is finite. In fact, it has a standard amplitude from 1 to 3eV [19]. This value is generally quite large as compared to typical electron and hole energies usually involved, so that the tunnel conductivity through the QD boundary is vanishingly small, except maybe for very small QDs. Actually, the electron or hole confinement energies increase as  $\propto R^{-2}$  for decreasing QD radius  $R$  and then should exceed the confinement potential step height for small QD sizes. Furthermore, the infinite potential well approximation implies that charge carriers inside the cluster are totally insensitive to its outside surroundings and also to any externally applied field, as far as considerations on QCSE are concerned. Although the surrounding effects may be sufficiently small to be neglected, the presence of a large external field can actually significantly modify the inside behavior of the micro-crystallites. Therefore, to justify the use of an infinite confining potential well, we have to take care of the electric field amplitude outside the QD, which should not exceed a certain threshold, fixed *ad hoc* by the height of the real confining potential step. This constraint should be referred to as the usual weak electric field limit. We will determine later an inequality, which analytically expresses the validity of this condition by linking the electric field amplitude to a certain number of other relevant physical parameters of the problem. It thus allows us to evaluate an approximate value for the maximal electric field amplitude we could apply on the QD, while still respecting the weak field limit.

Lastly, we should remind that for small nano-crystals of typical sizes of less than a hundred lattice spacings, there exist *magic numbers* for which clusters remain stable: *e.g.* crystalline silicon only stay coherent as clusters of  $Si_{12}$ ,  $Si_{33}$ ,  $Si_{39}$  and  $Si_{45}$ , if they contain less than 60 silicon atoms [50]. Their band structure should be deformed such that it becomes impossible to use the parabolic shape of conduction and valence bands,

on which the EMA-model is built. For sufficiently small electric field amplitude, it has been shown that, in semiconducting rectangular quantum boxes of typical size  $L \times W \times H$  as far as the weak field limit is concerned, the Stark shift of the confined exciton ground state presents essentially three contributions, each of them going as the fourth power of an edge length, *i.e.* the first scales as  $\propto L^4$ , the second as  $\propto W^4$  and the last as  $\propto H^4$  [34]. Thus, for a spherical potential well of radius  $R$ , the same Stark shift is expected to scale as  $\propto R^4$ . This is consistent with the physical fact that if there is no potential well — *i.e.* if there is no semiconductor micro-crystal embedded in the surrounding insulating matrix —, no electrons should be excited from the valence band to the conduction band, and no holes should then appear.

## 2.2. General considerations

Let  $V(r)$  be the confining potential well defined in spherical coordinates as:

$$V(\mathbf{r}) = V(r) = \begin{cases} 0 & \text{if } 0 \leq r \leq R, & \text{Region I;} \\ \infty & \text{if } r > R, & \text{Region II.} \end{cases}$$

Let  $V_C(\mathbf{r}_{\text{eh}})$  be the Coulomb interaction between electron and hole, in the single parabolic band approximation, the total electron-hole pair Hamiltonian operator reads (with  $\hbar = 1$ )

$$\begin{aligned} H_0 &= H_e + H_h + V_C(\mathbf{r}_{\text{eh}}) + E_g \\ &= -\frac{\nabla_e^2}{2m_e^*} - \frac{\nabla_h^2}{2m_h^*} + V(\mathbf{r}_e) + V(\mathbf{r}_h) - \frac{e^2}{\kappa r_{\text{eh}}} + E_g, \end{aligned} \quad (1)$$

where  $\kappa = 4\pi\varepsilon$ ,  $\varepsilon$  denotes the semiconductor dielectric constant,  $r_{\text{eh}} = |\mathbf{r}_{\text{eh}}| = |\mathbf{r}_e - \mathbf{r}_h|$  the electron-hole relative distance,  $m_{e,h}^*$  the effective mass and  $H_{e,h}$  the confinement Hamiltonian respectively of the electron and of the hole, and  $E_g$  the semiconductor energy band gap, which we will assume to be zero for convenience.

Without the Coulomb potential, the electron and the hole should be treated as decoupled particles, the QD wave function should be then factorized into separable electronic and hole parts  $\Psi(\mathbf{r}_e, \mathbf{r}_h) = \psi(\mathbf{r}_e)\psi(\mathbf{r}_h)$ . The orthonormal eigenfunctions  $\psi_{lnm}$  are labeled by three quantum numbers  $l \in \mathbb{N}$ ,  $n \in \mathbb{N}^* = \mathbb{N} - \{0\}$  and  $m \in \llbracket -l, l \rrbracket$ .

$$\begin{aligned} \psi_{lnm}(\mathbf{r}) &= \psi_{lnm}(r, \theta, \varphi) \\ &= \frac{\chi_{[0,R]}(r)}{R J_{\nu_l}'(k_{ln})} \sqrt{\frac{2}{r}} J_{\nu_l}\left(\frac{k_{ln}}{R} r\right) Y_l^m(\theta, \varphi), \end{aligned} \quad (2)$$

where

- $Y_l^m(\theta, \varphi)$  is the spherical harmonic of orbital quantum number  $l$  and azimuthal quantum number  $m$ ,
- $J_{\nu_l}(x)$  is the Bessel function of the first kind of index  $\nu_l = l + \frac{1}{2}$  and of variable  $x$ ,
- $\chi_{[0,R]}(r)$  is the characteristic function of radial interval,

- $\{k_{ln}\}_{ln}$  are the wave numbers in Region I defined as the  $n^{\text{th}}$  non-zero root of the Bessel function  $J_{\nu_l}(x)$  thanks to the continuity condition at  $r = R$ .

The respective energy eigenvalues for electron and hole are now expressed in terms of the same wave number set  $\{k_{ln}\}_{ln}$

$$E_{ln}^{\text{e,h}} = \frac{k_{ln}^2}{2m_{\text{e,h}}^* R^2}.$$

The continuum density of states of the semiconductor bulk should show atomic-like discrete spectrum with increasing energy separation as the radius decreases.

Because of the explicit micro-crystallites spherical shape symmetry breakdown in the presence of a Coulomb potential, which only depends in the electron-hole relative distance  $r_{\text{eh}}$ , the exact determination of eigenfunctions and energy eigenvalues for Eq. (1) is arduous. Treating the interplay of the Coulomb interaction, which scales as  $\propto R^{-1}$ , and the quantum confinement, which scales as  $\propto R^{-2}$ , constitutes the common approach to this problem. To handle these competing contributions, we should essentially distinguish two working regimes according to the ratio of the QD radius  $R$  to the Bohr radius of the bulk Mott-Wannier exciton  $a^* = \frac{\kappa}{e^2\mu}$ ,  $\mu$  being the reduced mass of the exciton:

- the strong confinement regime — valid for a size  $R \leq 2a^*$  [15] — in which the potential well strongly affects the relative electron-hole motion, the *exciton* states consist of uncorrelated electron and hole states;
- the weak confinement regime — valid for a size  $R \geq 4a^*$  [15] — in which the electron-hole relative motion and its binding energy are *quasi* left unchanged. The character of the exciton as a quasi-particle of total mass  $M = m_{\text{e}}^* + m_{\text{h}}^*$  is conserved, while its center-of-mass motion remains confined and should be quantized.

Even if we actually focus on Stark effect in the strong confinement regime, we shall briefly present the consequences of the previous single EMA-model in both strong confinement and weak confinement regimes. Despite the apparent simplicity of this model, it seems to be able to apprehend correctly QCSE, at least for a range of sufficiently small QD sizes, and to predict numerical values, which agree with experimental results.

### 2.3. Considerations on strong and weak confinement regimes

#### 2.3.1. Strong confinement regime

In this regime, the Coulomb potential is treated as a perturbation with respect to the infinite confinement potential well in a variational procedure, which shall be extended to the case of an applied electric field. In order to determine an approximate value for the ground state energy of the exciton state, we use the variational principle with the following trial wave function

$$\phi(\mathbf{r}_{\text{e}}, \mathbf{r}_{\text{h}}) = \psi_{010}(\mathbf{r}_{\text{e}})\psi_{010}(\mathbf{r}_{\text{h}})\phi_{\text{rel}}(\mathbf{r}_{\text{eh}}), \quad (3)$$

with  $\phi_{\text{rel}}(\mathbf{r}_{\text{eh}}) = \phi_{\text{rel}}(r_{\text{eh}}) = e^{-\frac{\sigma}{2}r_{\text{eh}}}$ , where  $\sigma$  denotes the variational parameter,  $r_{\text{e,h}} = |\mathbf{r}_{\text{e,h}}|$  and

$$\psi_{010}(\mathbf{r}_{\text{e,h}}) = \psi_{010}(r_{\text{e,h}}) = -\frac{\chi_{[0,R]}(r_{\text{e,h}})}{r_{\text{e,h}}\sqrt{2\pi R}} \sin\left(\frac{\pi}{R}r_{\text{e,h}}\right).$$

The variational wave function of Eq. (3) imposes that both electron and hole should occupy primarily their respective ground state in the confining infinite potential well, as described by the product wave function  $\psi_{010}(\mathbf{r}_{\text{e}})\psi_{010}(\mathbf{r}_{\text{h}})$ , and should exhibit, via the function  $\phi_{\text{rel}}(r_{\text{eh}})$  of the relative coordinates  $\mathbf{r}_{\text{eh}}$ , the exciton bound state behavior, analogous to the one found in a hydrogen-like atom with a mass  $\mu$ . Actually, this function  $\phi_{\text{rel}}(r_{\text{eh}})$  describes the excitonic contribution of the ground state as an hydrogen-like atom with an appropriate Bohr radius, up to a normalization factor, especially if we expect that  $\sigma^{-1} \propto a^*$ .

Despite the fact that the spherical confining potential well breaks the translation invariance of the Coulomb interaction, Fourier transform formalism in relative electron-hole coordinates allows to establish integral representations for quantities such as the square of the norm of the trial function  $\phi(\mathbf{r}_{\text{e}}, \mathbf{r}_{\text{h}})$  or the corresponding Coulomb potential diagonal matrix element (*cf.* Appendix A for details)

$$\left\{ \begin{array}{l} \langle \phi | \phi \rangle = -\frac{8}{R^2} \partial_{\sigma} \frac{1}{\sigma} \iint_{\mathcal{D}} \frac{dx dy}{x y} \sin^2(\pi x) \sin^2(\pi y) \sinh(\sigma R x) e^{-\sigma R y}, \\ \langle \phi | V_{\text{C}}(r_{\text{eh}}) | \phi \rangle = -\frac{e^2}{\kappa R} \frac{8}{\sigma} \iint_{\mathcal{D}} \frac{dx dy}{x y} \sin^2(\pi x) \sin^2(\pi y) \sinh(\sigma R x) e^{-\sigma R y}, \end{array} \right. \quad (4)$$

where  $\mathcal{D} = \{(x, y) \in \mathbb{R}^2 / 0 \leq x \leq y \leq 1\}$ .

A Taylor expansion of expressions (4) with respect to the dimensionless parameter  $\sigma R$  near zero yields

$$\left\{ \begin{array}{l} \langle \phi | \phi \rangle = 1 - B\sigma R + O(\sigma^2 R^2), \\ \langle \phi | V_{\text{C}}(r_{\text{eh}}) | \phi \rangle = -\frac{e^2}{\kappa R} \{A - \sigma R + O(\sigma^2 R^2)\}. \end{array} \right.$$

Thus, an expression of the mean value of the total Hamiltonian  $H_0$  in the strong confinement regime in terms of a dimensionless variational parameter  $\sigma'$ , defined by  $\sigma' = \sigma a^*$ , and of the binding exciton Rydberg energy  $E^* = \frac{1}{2\mu a^{*2}}$  can be obtained as

$$\frac{\langle \phi | H_0 | \phi \rangle}{\langle \phi | \phi \rangle} = \frac{\pi^2}{2\mu R^2} - A \frac{e^2}{\kappa R} - 2B' E^* \sigma' + \frac{E^*}{4} \sigma'^2 + \dots$$

where the correction terms “...” go to zero as soon as  $\frac{R}{a^*}$  goes to zero §. The variational parameter  $\sigma'$  is now determined by minimizing the expectation value of the electron-hole

§ Any constant, which is introduced but not explicitly defined in the article, is actually presented in Appendix B.



energy. Then, its value is found to be  $\sigma'_0 = 4B' \approx 0.9956$  and the corresponding value of the energy is

$$E_{\text{eh}}^{\text{strong}} = E_{\text{eh}} - A \frac{e^2}{\kappa R} - 4B'^2 E^*,$$

where  $E_{\text{eh}} = \frac{\pi^2}{2\mu R^2}$  is the electron-hole pair ground state confinement energy. In the strong confinement regime, this formula has been already analytically obtained in [15,51] with trial functions showing the same global form as  $\phi(\mathbf{r}_e, \mathbf{r}_h)$ , but with an interactive part equal to  $\tilde{\phi}_{\text{rel}}(\mathbf{r}_{\text{eh}}) = (1 - \frac{\sigma}{2} r_{\text{eh}})$ , instead of  $\phi_{\text{rel}}(\mathbf{r}_{\text{eh}})$ . It is obvious that  $\tilde{\phi}_{\text{rel}}(\mathbf{r}_{\text{eh}})$  consists of the two first terms of the Taylor expansion of  $\phi_{\text{rel}}(\mathbf{r}_{\text{eh}})$ , in the limit  $\frac{\sigma}{2} r_{\text{eh}} \leq \sigma R \ll 1$ . Because of the infinite potential well confinement assumption, the total excitonic energy is actually overestimated in comparison to experimental data for small QDs. A standard successful method to subtract off this over-estimation consists in adopting a model in which we restore a confining finite potential step of experimentally acceptable height, this approach actually leads to a significantly better fit of the experimental data [19].

### 2.3.2. Weak confinement regime

In this regime, electron-hole pair states should consist of electron-hole pair bound states. The Coulomb potential and the kinetic energy in the electron-hole relative coordinates should be of the same order of magnitude because the QD size authorizes a partial restoration of the long range Coulomb interaction between the charged carriers inside the QD. Then, the most important contribution to the ground state energy of the exciton should be the ground state of a hydrogen-like atom with an appropriate reduced mass  $\mu$ . Therefore, in the weak confinement regime, the leading term of the excitonic total energy is of the order of  $-E^*$ . Furthermore, we should remark that this contribution accounts for the total energy in the exciton relative coordinates, because of the validity of the Virial theorem in this set of coordinates. Finally, the total translational motion of the exciton, thought as a quasi-particle of total mass  $M$ , should be restored and contributes to the exciton total energy by the typical kinetic energy term of a free particle, confined in a space region of size  $R$ , *i.e.* by  $\frac{\pi^2}{2MR^2}$ . As a first approximation, we compute the total exciton ground state energy in the weak confinement regime by adding two energetic contributions from two different properties of the exciton trapped inside the QD

$$E_{\text{eh}}^{\text{weak}} = -E^* + \frac{\pi^2}{2MR^2}.$$

Actually, the previous formula is not totally satisfactory. To improve phenomenologically its accuracy in regard to empirical data from numerical simulations, a monotonic increasing function  $\eta(\lambda)$  of the effective masses ratio  $\lambda = \frac{m_{\text{h}}^*}{m_{\text{e}}^*}$  has been defined by [15], and has been inserted into  $E_{\text{eh}}^{\text{weak}}$  as follows

$$E_{\text{eh}}^{\text{weak}} = -E^* + \frac{\pi^2}{2M(R - \eta(\lambda)a^*)^2}.$$

The QD size *renormalization* term  $\eta(\lambda)a^*$  is interpretable as a dead layer [52]. This is the physical reminiscence of the fact that, although it could be successfully described as a quasi-particle, the exciton is not actually itself an indivisible particle. Its center-of-mass motion, the one on which the quantization is really performed, could not reach the infinite potential well surface unless the exciton undergoes a strong deformation in the relative motion of the electron and the hole. This implies that the picture of a point-like exciton should be dropped in this region of space. The exciton should be preferentially thought as a rigid sphere of radius  $\propto a^*$ . The proportionality factor is, in practice, numerically determined in order to get a better fit of experimental results. It must not significantly exceed  $\frac{3}{2}$ , because  $l^* = \frac{3}{2}a^*$  is the mean value of the relative distance between the electron and the hole in the non-confined exciton ground state.

### 3. Stark effect without polarization energy

The calculation of the eigenfunctions and energy eigenvalues of electron-hole pair trapped in an infinite potential well QD and under the influence of an external constant electric field is, in principle, an exactly solvable problem. However, the presence of a constant electric field explicitly breaks both spherical QD symmetry and electron-hole Coulomb potential translation invariance.

Consider now an applied electric field  $\mathbf{E}_a$  along the direction  $z$  of a three-dimensional cartesian coordinates system with its origin located at the QD center. Because the dielectric constant  $\varepsilon$  of the inside semiconducting QD is larger than the dielectric constant  $\varepsilon'$  of the outside insulating matrix, the electric field  $\mathbf{E}_d$  inside the QD is actually different from the one externally applied. It should be then reduced, according to [53], as  $\mathbf{E}_d = \frac{\mathbf{E}_a}{(1-g) + g\varepsilon_r}$ , where  $g$  is a geometrical depolarization factor, which equals  $\frac{1}{3}$  for a sphere, and where  $\varepsilon_r = \frac{\varepsilon}{\varepsilon'}$  is defined as the relative dielectric constant. Moreover, the difference between the dielectric constants inside and outside micro-crystals also implies the existence of a polarization energy term  $P(\mathbf{r}_e, \mathbf{r}_h)$ , introduced by Brus [8], which shall be dropped first in this section, but taken into account in the next one. This methodology allows us to study in more details its relative role *vs.* the Coulomb potential because they both typically scale as  $\propto R^{-1}$  and, consequently, they should contribute to the exciton total energy with terms of the same order of magnitude.

For the moment, let us simply define the electron and the hole (of respective electric charge  $\mp e$ ) interaction Hamiltonian under an electric field inside the nano-crystal. Their expression in spherical coordinates is

$$W_{e,h}(\mathbf{r}_{e,h}) = \pm e \mathbf{E}_d \cdot \mathbf{r}_{e,h} = \pm e E_d r_{e,h} \cos \theta_{e,h}, \quad (5)$$

where  $E_d = |\mathbf{E}_d|$  is the electric field amplitude inside the micro-crystal. In order to justify an appropriate form for the trial wave function, we note that the function  $\phi(\mathbf{r}_e, \mathbf{r}_h)$  introduced in Eq. (3) does not provide any further contribution to the excitonic energy in the presence of the electric field, *i.e.*  $\langle \phi | W_e(\mathbf{r}_e) | \phi \rangle = -\langle \phi | W_h(\mathbf{r}_h) | \phi \rangle$ . Therefore, the

variational function should present some other dependence on the electron and hole space coordinates to be determined later.

### 3.1. Justification of the variational trial wave function form

To apprehend the effect of the induced electric polarization, we follow a reasoning made in [39], by studying the interaction between the electron (resp. the hole) with the ambient electric field and neglecting the Coulomb potential. To this end, let us define the individual Hamiltonian  $H'_e$  (resp.  $H'_h$ ) of confined electron (resp. of confined hole) interacting with a constant electric field  $\mathbf{E}_d$  as

$$\begin{aligned} H'_{e,h} &= H_{e,h} + W_{e,h}(\mathbf{r}_{e,h}) \\ &= -\frac{\nabla_{e,h}^2}{2m_{e,h}^*} + V(\mathbf{r}_{e,h}) + W_{e,h}(\mathbf{r}_{e,h}). \end{aligned}$$

As mentioned as a consistency condition in Subsection 2.1, we can assume that the electric field amplitude is sufficiently small so as to consider the Hamiltonian interactive part  $W_{e,h}(\mathbf{r}_{e,h})$  as a perturbation to the confined Hamiltonian  $H_{e,h}$ . In this weak field limit, for which the perturbation point of view should hold, the typical interaction energy of the electron (resp. of the hole) under the electric field influence should be treated as a perturbation compared to their typical confinement energy

$$E_{\text{ele}} \ll E_{e,h},$$

where we define  $E_{e,h} = E_{01}^{e,h}$  to simplify the notations. The energy  $E_{\text{ele}} = eE_d R$  is introduced as in the absolute value of the typical energy due to the interaction of the electron (resp. of the hole) with the applied electric field inside the QD. In real atoms, Stark shifted levels show a typical dependence on the electric field of the form  $\propto E_d^2$ . A similar behavior is expected here.

In the following, in order to justify the form of the parts we should add to the electron-hole variational wave function  $\phi(\mathbf{r}_e, \mathbf{r}_h)$  to efficiently come up with QCSE, we will first investigate perturbative results of decoupled confined electron and hole, which interact individually with an external electric field. The interaction Hamiltonian  $W_{e,h}(\mathbf{r}_{e,h})$  describing the electron and the hole into the electric field is treated as a perturbation of their respective confinement Hamiltonian  $H_{e,h}$  by performing, on one hand, a standard second-order stationary perturbation theory and, on the other hand, by a variational procedure.

**Stationary perturbation principle.** A second-order perturbation procedure gives the expectation value of the ground state perturbed energy  $E'_{e,h}$  of the confined electron (or of the confined hole) in the presence of an electric field and the corresponding

wave function  $\Psi_{e,h}(\mathbf{r}_{e,h})$  in Dirac notation as

$$\left\{ \begin{array}{l} E'_{e,h} = E_{e,h} + e^2 E_d^2 \sum_{\substack{lnm \\ (l,n) \neq (0,1)}} \frac{|\langle \psi_{lnm} | r \cos \theta | \psi_{010} \rangle|^2}{E_{e,h} - E_{ln}^{e,h}} + O(E_d^3), \\ |\Psi_{e,h}\rangle = |\psi_{010}\rangle \pm e E_d \sum_{\substack{lnm \\ (l,n) \neq (0,1)}} \frac{\langle \psi_{lnm} | r \cos \theta | \psi_{010} \rangle}{E_{e,h} - E_{ln}^{e,h}} |\psi_{lnm}\rangle + O(E_d^2). \end{array} \right.$$

After computing the matrix elements  $\langle \psi_{lnm} | r \cos \theta | \psi_{010} \rangle$  for  $l \in \mathbb{N}$ ,  $n \in \mathbb{N}^*$  and  $m \in \llbracket -l, l \rrbracket$  (cf. Appendix C for details), we deduce the Stark shift undergone by the electron (or by the hole) ground state, up to the second order in the electric field amplitude,

$$\Delta E_{e,h}^{\text{Stark pert}} = E'_{e,h} - E_{e,h} = -\Gamma_{\text{pert}} m_{e,h}^* e^2 E_d^2 R^4 + O(E_d^3),$$

where the constant  $\Gamma_{\text{pert}}$  has the value

$$\Gamma_{\text{pert}} = \frac{32}{3} \pi^2 \sum_{n \geq 1} \frac{k_{1n}^2}{(k_{1n}^2 - \pi^2)^5} \approx 0.01817.$$

**Variational principle.** In order to account for the electric field direction along the  $z$ -axis in the variational principle, the trial wave function should show deformation away from the spherical shape, which squeezes or stretches the electron or the hole probability density along this particular direction. Then, the variational trial function should be chosen of the form

$$\Phi_{e,h}(\mathbf{r}_{e,h}) = \psi_{010}(\mathbf{r}_{e,h}) \varphi_{e,h}(\mathbf{r}_{e,h}),$$

where  $\varphi_{e,h}(\mathbf{r}_{e,h}) = e^{\mp \frac{\sigma_{e,h}}{2} r_{e,h} \cos \theta_{e,h}}$ . The variational parameters  $\sigma_{e,h}$  have the dimension of an inverse length so that, in the weak field approximation, we can assume  $\sigma_{e,h} R \ll 1$ . The computational difficulty of this problem is therefore contained in the calculation of the square of the norm of the trial function  $\Phi_{e,h}(\mathbf{r}_{e,h})$ , which admits an integral representation. By performing a Taylor expansion on this expression in the neighborhood of the dimensionless parameter  $\sigma_{e,h} R = 0$ , we deduce

$$\begin{aligned} \langle \Phi_{e,h} | \Phi_{e,h} \rangle &= \frac{2}{\sigma_{e,h} R} \int_0^1 \frac{dx}{x} \sin^2(\pi x) \sinh(\sigma_{e,h} R x) \\ &= 1 + \frac{C}{6} \sigma_{e,h}^2 R^2 + O(\sigma_{e,h}^4 R^4) \\ &= 1 + O(\sigma_{e,h}^2 R^2). \end{aligned}$$

Moreover, we can exactly determine the mean value of the electric field free confinement Hamiltonian  $H_{e,h}$  in the quantum state defined by the trial function  $\Phi_{e,h}(\mathbf{r}_{e,h})$

$$\frac{\langle \Phi_{e,h} | H_{e,h} | \Phi_{e,h} \rangle}{\langle \Phi_{e,h} | \Phi_{e,h} \rangle} = E_{e,h} + \frac{\sigma_{e,h}^2}{8m_{e,h}^*},$$

and we can also evaluate the mean value of the interaction Hamiltonian  $W_{e,h}(\mathbf{r}_{e,h})$  by using the previous Taylor expansion for  $\langle \Phi_{e,h} | \Phi_{e,h} \rangle$

$$\begin{aligned} \frac{\langle \Phi_{e,h} | W_{e,h} | \Phi_{e,h} \rangle}{\langle \Phi_{e,h} | \Phi_{e,h} \rangle} &= \pm eE_d \frac{\langle \Phi_{e,h} | r_{e,h} \cos \theta_{e,h} | \Phi_{e,h} \rangle}{\langle \Phi_{e,h} | \Phi_{e,h} \rangle} \\ &= -eE_d \partial_{\sigma_{e,h}} \log \langle \Phi_{e,h} | \Phi_{e,h} \rangle \\ &= -e\sigma_{e,h} E_d R^2 \left\{ \frac{C}{3} + O(\sigma_{e,h}^2 R^2) \right\}. \end{aligned}$$

Then, we obtain the total Hamiltonian  $H'_{e,h}$  mean value as an expansion up to the second order in the dimensionless parameter  $\sigma_{e,h}R$

$$\frac{\langle \Phi_{e,h} | H'_{e,h} | \Phi_{e,h} \rangle}{\langle \Phi_{e,h} | \Phi_{e,h} \rangle} = E_{e,h} + \frac{\sigma_{e,h}^2}{8m_{e,h}^*} - \frac{C}{3} eE_d R^2 \sigma_{e,h} + \dots,$$

on which we shall apply the variational principle. The correct variational parameter value is  $\sigma_{e,h}^0 = \frac{4C}{3} m_{e,h}^* eE_d R^2$ . It minimizes the ground state energy  $E'_{e,h}$  of the electron (or of the hole) interaction with the electric field and we get the Stark shift by subtracting the confined electron (or hole) ground state energy as follows

$$\Delta E_{\text{Stark var}}^{e,h} = E'_{e,h} - E_{e,h} = -\Gamma_{\text{var}} m_{e,h}^* e^2 E_d^2 R^4,$$

where  $\Gamma_{\text{var}} = \frac{2C^2}{9} \approx 0.01776$ .

We observe that the two Stark shift expressions present the same dependence on the physical parameters of the problem under study, they both scale as  $\propto m_{e,h}^* e^2 E_d^2 R^4$ . Furthermore, we could easily establish that the Stark shift contribution is actually a second order term in the dimensionless parameter  $\frac{E_{\text{ele}}}{E_{e,h}} \ll 1$ , with respect to the electron or the hole confinement energy  $E_{e,h}$ ,

$$\Delta E_{\text{Stark}}^{e,h} = -\Gamma m_{e,h}^* e^2 E_d^2 R^4 = -\Gamma \frac{\pi^2}{2} \frac{E_{\text{ele}}^2}{E_{e,h}^2} E_{e,h},$$

where the constant  $\Gamma$  stands for either  $\Gamma_{\text{pert}}$  or  $\Gamma_{\text{var}}$ , according to the corresponding cases. The multiplicative factor  $\Gamma \frac{\pi^2}{2}$ , which naturally appears, takes, for both perturbation procedures, a value of order around 0.09. Finally, the difference between the two different methods we use is quantifiable by evaluating the relative error between the values of the proportionality constants  $\Gamma_{\text{pert}}$  and  $\Gamma_{\text{var}}$ , which is around 2%. This relative error supports the validity of the new trial wave function  $\Phi(\mathbf{r}_e, \mathbf{r}_h)$  in the presence of the electric field, defined as

$$\Phi(\mathbf{r}_e, \mathbf{r}_h) = \phi(\mathbf{r}_e, \mathbf{r}_h) \varphi_e(\mathbf{r}_e) \varphi_h(\mathbf{r}_h). \quad (6)$$

It is reasonable to assume that this variational function presents the necessary properties to describe the QCSE in spherical semiconductor QDs. It possesses, on one hand, a part  $\phi(\mathbf{r}_e, \mathbf{r}_h)$  describing the Coulomb interaction between the electron and hole both occupying the ground state of their respective confinement Hamiltonian and, on the other hand, the electric field interactive part  $\varphi_e(\mathbf{r}_e) \varphi_h(\mathbf{r}_h)$  liable for the individual electron and hole behaviors in an ambient electric field inside the micro-crystal.

### 3.2. General results on Stark effect in semiconductor Quantum Dots

As already mentioned, we add the interaction Hamiltonian  $W_{e,h}(\mathbf{r}_{e,h})$  between the electron (or the hole) and the electric field to the QD model Hamiltonian  $H_0$ , introduced in Section 2, in order to apprehend QCSE in semiconductor micro-crystals with spherical shape. Thus,

$$H = H_0 + W_e(\mathbf{r}_e) + W_h(\mathbf{r}_h). \quad (7)$$

In the limit of weak electric fields, we would apply the variational procedure on the trial function  $\Phi(\mathbf{r}_e, \mathbf{r}_h)$ , introduced in Eq. (6). To this end, we shall use a reasoning similar to that of Subsection 2.2, *i.e.* the Fourier transform formalism in the relative coordinates can be used once again quite advantageously. This formalism leads to integral representation of the square of the norm of the trial function  $\Phi(\mathbf{r}_e, \mathbf{r}_h)$  and of the mean value of the Coulomb interaction matrix element in the corresponding quantum state (*cf.* Appendix A for details)

$$\left\{ \begin{array}{l} \langle \Phi | \Phi \rangle = -\frac{2}{R^2} \partial_\sigma \frac{1}{\sigma} \int_{-1}^1 d\xi \iint_{\mathcal{D}} \frac{dx}{x} \frac{dy}{y} \sin^2(\pi x) \sin^2(\pi y) \\ \quad \times \left\{ \frac{\sinh(\rho_e(\xi)\sigma R x)}{\rho_e(\xi)} \frac{e^{-\rho_h(\xi)\sigma R y}}{\rho_h(\xi)} + \frac{\sinh(\rho_h(\xi)\sigma R x)}{\rho_h(\xi)} \frac{e^{-\rho_e(\xi)\sigma R y}}{\rho_e(\xi)} \right\}, \\ \langle \Phi | V_C(r_{eh}) | \Phi \rangle = -\frac{e^2}{\kappa R} \frac{2}{\sigma R} \int_{-1}^1 d\xi \iint_{\mathcal{D}} \frac{dx}{x} \frac{dy}{y} \sin^2(\pi x) \sin^2(\pi y) \\ \quad \times \left\{ \frac{\sinh(\rho_e(\xi)\sigma R x)}{\rho_e(\xi)} \frac{e^{-\rho_h(\xi)\sigma R y}}{\rho_h(\xi)} + \frac{\sinh(\rho_h(\xi)\sigma R x)}{\rho_h(\xi)} \frac{e^{-\rho_e(\xi)\sigma R y}}{\rho_e(\xi)} \right\}, \end{array} \right. \quad (8)$$

where the functions  $\rho_{e,h}(\xi)$  are defined as

$$\rho_{e,h}(\xi) = \sqrt{1 - 2\frac{\sigma_{e,h}}{\sigma}\xi + \frac{\sigma_{e,h}^2}{\sigma^2}}, \quad -1 \leq \xi \leq 1.$$

According to Appendix A, we note that Eqs. (8) are valid if and only if the different variational parameters  $\sigma$  and  $\sigma_{e,h}$  satisfy the inequality

$$0 \leq e\sigma_{e,h} < \sigma, \quad (9)$$

where  $e = \exp(1)$ . This condition on different variational parameters is a consistency condition, which analytically determines the range of acceptable electric field amplitudes. As matter of fact, on one hand, following the variational results for the interaction between the electric field with the electron (or with the hole), we expect that  $\sigma_{e,h}$  should scale as  $\propto m_{e,h}^* e E_d R^2$  and, on the other hand, following the variational results on the electric field free interactive electron-hole pair through the Coulomb potential, we also expect that  $\sigma \propto a^{*-1}$ . Therefore, after performing some simple rearrangements, Eq. (9) provides a validity criterion in terms of different typical electron (or hole) energy, because  $\frac{\sigma_{e,h}}{\sigma} \propto \frac{E_{ele} a^*}{E_{e,h} R}$ . This dependence naturally justifies

the fact that the weak field limit should remain valid if the ratio  $\frac{E_{\text{ele}}}{E_{\text{e,h}}}$  does not exceed, up to a dimensionless proportionality factor to be given later, the order of magnitude of the ratio  $\frac{R}{a^*}$ , the quantity which characterizes the strong confinement regime. The electron (resp. the hole) energy, in the presence of the electric field, should be at most of the same order of magnitude of a first term correction to the electron (resp. the hole) confinement energy in the strong confinement regime, which corresponds to the absolute value of the typical energetic contribution of the electron-hole Coulomb interaction — they actually both scale as  $\propto R^{-1}$ .

Moreover, in the limit of weak electric field, based on the decoupled electron-hole point of view presented in Subsection 3.1, we also reasonably expect that the Stark shift for the coupled electron-hole system should scale as

$$\propto (m_e^* + m_h^*)e^2 E_d^2 R^4 \propto \left\{ \frac{E_{\text{ele}}^2}{E_e^2} E_e + \frac{E_{\text{ele}}^2}{E_h^2} E_h \right\} \propto E_{\text{eh}} \frac{R^2}{a^{*2}}.$$

Then, in order to get at least the lowest order contribution to the Stark shift in the strong confinement, it is necessary to perform a Taylor expansion of the total Hamiltonian  $H$  mean value up at least to the second order in the variational parameters. However, as we shall see in the following subsection, this first contribution is not sufficiently accurate to fit experimental data because it does not account for the coupling between the electron and the hole through the Coulomb interaction. This is the reason why we shall carry on the expansion up to the third order, since we will also get the first correction in  $\frac{\tilde{R}}{a^*}$  to the Stark shift, which explicitly expresses the presence of the Coulomb potential in the strong confinement regime.

Furthermore, Eq. (9) indicates approximate boundaries values for the previous quantities  $\rho_{\text{e,h}}(\xi)$ . Actually, we straightforwardly deduce, for  $-1 \leq \xi \leq 1$ , that

$$\frac{1}{2} < 1 - \frac{1}{e} < 1 - \frac{\sigma_{\text{e,h}}}{\sigma} \leq \rho_{\text{e,h}}(\xi) \leq 1 + \frac{\sigma_{\text{e,h}}}{\sigma} < 1 + \frac{1}{e} < \frac{3}{2}.$$

In the limit of vanishing electric field, *i.e.* in the limit  $\frac{\sigma_{\text{e,h}}}{\sigma} \rightarrow 0$ , the expressions in Eqs. (8) allow us to retrieve the expressions for the square of the norm and for the Coulomb potential mean value without electric field expressed by Eq. (4).

Finally, we shall obtain the interaction Hamiltonian  $W_{\text{e,h}}(\mathbf{r}_{\text{e,h}})$  mean value from the square of the norm of the wave function  $\Phi(\mathbf{r}_{\text{e}}, \mathbf{r}_{\text{h}})$  by taking its logarithmic derivative with respect to the variational parameters  $\sigma_{\text{e,h}}$

$$\frac{\langle \Phi | W_{\text{e,h}}(\mathbf{r}_{\text{e,h}}) | \Phi \rangle}{\langle \Phi | \Phi \rangle} = -e E_d \partial_{\sigma_{\text{e,h}}} \log \langle \Phi | \Phi \rangle. \quad (10)$$

We are also able to conduct the computation of the exact mean value of the electric field free Hamiltonian  $H_0$

$$\frac{\langle \Phi | H_0 | \Phi \rangle}{\langle \Phi | \Phi \rangle} = E_{\text{eh}} + \frac{\sigma^2}{8\mu} + \frac{\sigma_e^2}{8m_e^*} + \frac{\sigma_h^2}{8m_h^*}. \quad (11)$$

As we have build the trial function  $\Phi(\mathbf{r}_e, \mathbf{r}_h)$ , so that it possesses the properties of the functions  $\phi(\mathbf{r}_e, \mathbf{r}_h)$  and  $\Phi_{e,h}(\mathbf{r}_{e,h})$ , we should expect that the same goes for the mean value of the confinement Hamiltonian  $H_0$ . This quantity should contain at least the electron-hole pair ground state confinement energy  $E_{eh}$ , due to the presence of the function  $\psi_{010}(\mathbf{r}_e)\psi_{010}(\mathbf{r}_h)$ , the contributions to the total kinetic energy  $\frac{\sigma^2}{8\mu}$ , due to the Coulomb potential, and  $\frac{\sigma_{e,h}^2}{8m_{e,h}^*}$ , due to the interaction between the charge carriers and the electric field. However, in addition to the four previous expected terms, direct calculations exhibit a further contribution to the mean value of  $H_0$  of the form

$$\frac{K_h(\sigma, \sigma_e, \sigma_h)}{2m_h^* \langle \Phi | \Phi \rangle} - \frac{K_e(\sigma, \sigma_e, \sigma_h)}{2m_e^* \langle \Phi | \Phi \rangle},$$

where the functions  $K_{e,h}(\sigma, \sigma_e, \sigma_h)$  are given by

$$\begin{aligned} & K_{e,h}(\sigma, \sigma_e, \sigma_h) \\ &= \mp \int_{(\mathbb{R}^3)^2} d^3\mathbf{r}_e d^3\mathbf{r}_h \psi_{010}^2(\mathbf{r}_e) \psi_{010}^2(\mathbf{r}_h) \varphi_{h,e}^2(\mathbf{r}_{h,e}) \left[ \nabla \phi_{rel}^2(\mathbf{r}_{eh}) \right] \cdot [\varphi_{e,h}(\mathbf{r}_{e,h}) \nabla \varphi_{e,h}(\mathbf{r}_{e,h})] \\ &= \frac{\sigma \sigma_{e,h}}{2} \{ \partial_{\sigma_e} + \partial_{\sigma_h} \} \langle \Phi | \frac{1}{|\mathbf{r}_{eh}|} | \Phi \rangle. \end{aligned}$$

Real physical quantities should be invariant under the electron-hole exchange symmetry defined by the exchange of their coordinates, their masses and their electric charges

$$\begin{cases} \mathbf{r}_{e,h} & \longrightarrow \mathbf{r}_{h,e}, \\ m_{e,h}^* & \longrightarrow m_{h,e}^*, \\ e & \longrightarrow -e. \end{cases} \quad (12)$$

As we expect that  $\sigma_{e,h} \propto m_{e,h}^* e E_d R^2$ , under an electron-hole exchange, the variational parameters should transform as  $\sigma_{e,h} \longrightarrow -\sigma_{h,e}$ . Therefore, the trial function  $\Phi(\mathbf{r}_e, \mathbf{r}_h)$ , the confinement Hamiltonian  $H_0$ , the Coulomb potential  $V_C(r_{eh})$  and the interaction Hamiltonian  $W_e(\mathbf{r}_e) + W_h(\mathbf{r}_h)$  remain actually invariant under the electron-hole exchange, as well as the norm of  $\Phi(\mathbf{r}_e, \mathbf{r}_h)$  and the mean value of these operators. But, the next contribution will not. As a matter of fact, it verifies

$$\left[ \frac{K_h(\sigma, \sigma_e, \sigma_h)}{2m_h^* \langle \Phi | \Phi \rangle} - \frac{K_e(\sigma, \sigma_e, \sigma_h)}{2m_e^* \langle \Phi | \Phi \rangle} \right] \longrightarrow \left[ \frac{K_e(\sigma, \sigma_e, \sigma_h)}{2m_e^* \langle \Phi | \Phi \rangle} - \frac{K_h(\sigma, \sigma_e, \sigma_h)}{2m_h^* \langle \Phi | \Phi \rangle} \right].$$

Then, because of the mean value of the confinement Hamiltonian  $H_0$  invariance, it should not bring any new contribution to real physical quantities and should be immediately discarded from  $\frac{\langle \Phi | H_0 | \Phi \rangle}{\langle \Phi | \Phi \rangle}$ , which should be now exactly expressed as given by Eq. (11).

### 3.3. Stark effect in strong confinement regime

As there seems to be no way to analytically compute the integrals in Eqs. (8), we shall Taylor expand them in the strong confinement regime, *i.e.* when  $\sigma R \ll 1$ . In order to



perform this expansion, we have to specify the QD radii region, in which the following expressions are valid in the strong confinement region. For this, we shall assume that the quantities  $\rho_{e,h}(\xi)\sigma R$  in the arguments of the functions  $\exp(x)$  and  $\sinh(x)$ , appearing in Eq. (8) should be sufficiently small. This is the reason why we will only consider the range of QD radii such that  $R \leq \frac{2}{3\sigma'}a^*$ , where the dimensionless variational parameter  $\sigma'$  should take its variational value. From the bounds of the functions  $\rho_{e,h}(\xi)$ , we derive the following bounds for  $\rho_{e,h}(\xi)\sigma Rx, \rho_{e,h}(\xi)\sigma Ry \lesssim 1$ , if  $-1 \leq \xi \leq 1$  and  $0 \leq x \leq y \leq 1$ . Moreover, since different variational parameters  $\sigma$  and  $\sigma_{e,h}$  can be of the same order of magnitude, because of the consistency condition (9), we deduce, up to the third order in  $\sigma R$ , that

$$\left\{ \begin{array}{l} \langle \Phi | \Phi \rangle = 1 - B\sigma R + C\sigma^2 R^2 - D\sigma^3 R^3 \\ \quad + (C - D'\sigma R)\frac{\sigma_e^2 + \sigma_h^2}{6}R^2 - D''\sigma\sigma_e\sigma_h R^3 + O(\sigma^4 R^4), \\ \frac{\langle \Phi | V_C(r_{eh}) | \Phi \rangle}{\langle \Phi | \Phi \rangle} = \frac{-e^2}{\kappa R} \left\{ A + B'\sigma R + C'\sigma^2 R^2 + C'_1(\sigma_e^2 + \sigma_h^2)R^2 \right. \\ \quad \left. + C'_2\sigma_e\sigma_h R^2 + O(\sigma^3 R^3) \right\}, \\ \frac{\langle \Phi | W_{e,h}(r_{e,h}) | \Phi \rangle}{\langle \Phi | \Phi \rangle} = -eE_d R \left[ \left\{ C + (BC - D')\sigma R \right\} \frac{\sigma_{e,h}R}{3} - D''\sigma_{h,e}\sigma R + O(\sigma^3 R^3) \right]. \end{array} \right. \quad (13)$$

The mean value of the total Hamiltonian  $H$ , under the influence of the electric field on both electron and hole is then expressed as an expansion in powers of the variational parameters, up to third order,

$$\begin{aligned} \frac{\langle \Phi | H | \Phi \rangle}{\langle \Phi | \Phi \rangle} &= E_{eh} - A\frac{e^2}{\kappa R} + \frac{E^*}{4}\sigma'^2 + \frac{\sigma_e^2}{8m_e^*} + \frac{\sigma_h^2}{8m_h^*} - 2B'E^*\sigma' \\ &\quad - 2C'E^*\frac{R}{a^*}\sigma'^2 - C'_1\frac{\sigma_e^2 + \sigma_h^2}{\mu}\frac{R}{a^*} - C'_2\frac{\sigma_e\sigma_h}{\mu}\frac{R}{a^*} \\ &\quad - eE_d(\sigma_e + \sigma_h)R^2 \left\{ \frac{C}{3} - C''\frac{R}{a^*}\sigma' \right\} + \dots \end{aligned} \quad (14)$$

Applying now the variational procedure, we minimize the previous matrix element with respect to  $\sigma'$  and  $\sigma_{e,h}$  to obtain an approximate value of the ground state total energy. Thus, their values are determined to the first order in  $\frac{R}{a^*}$  to insure the coherence of the expansion we made and to account for all contributions to the ground state energy

$$\left\{ \begin{array}{l} \sigma'_0 = 4B' \left\{ 1 + 8C'\frac{R}{a^*} \right\} - 8\frac{CC''}{3}(m_e^* + m_h^*)\frac{e^2 E_d^2 R^4}{E^* a^*}, \\ \sigma_{e,h}^0 = \frac{4C}{3}m_{e,h}^* eE_d R^2 \left\{ 1 + 4\Sigma_{e,h}\frac{R}{a^*} \right\}, \end{array} \right. \quad (15)$$

where  $\Sigma_{e,h} = \frac{1}{\mu} \left\{ 2C'_1 + C'_2\frac{m_{h,e}^*}{m_{e,h}^*} \right\} - \frac{3B'C''}{Cm_{e,h}^*}$  and

$$\begin{aligned} E'_{eh} &= E_{eh} - A\frac{e^2}{\kappa R} - 4B'^2 \left\{ 1 + 8C'\frac{R}{a^*} \right\} E^* - \Gamma_{\text{var}}(m_e^* + m_h^*)e^2 E_d^2 R^4 \\ &\quad - 8\Gamma_{\text{var}}e^2 E_d^2 R^4 \left\{ C'_1\frac{m_e^{*2} + m_h^{*2}}{\mu} + C'_2\frac{m_e^*m_h^*}{\mu} - \frac{3B'C''}{C}(m_e^* + m_h^*) \right\} \frac{R}{a^*}. \end{aligned} \quad (16)$$

The previous expression allows us to identify the Stark shift in the strong confinement regime as terms scaling as  $\propto E_d^2$ , *i.e.*

$$\Delta E_{\text{Stark}}^{\text{strong}} = -\Gamma_{\text{var}}(m_e^* + m_h^*)e^2 E_d^2 R^4 \left\{ 1 + 8\Gamma_{\text{var}}^{\text{eh}} \frac{R}{a^*} \right\}, \quad (17)$$

where  $\Gamma_{\text{var}}$  appears as of universal character, while the constant  $\Gamma_{\text{var}}^{\text{eh}}$  depends on the semiconductor. In terms of the effective masses of the electron and the hole, it can be expressed as

$$\Gamma_{\text{var}}^{\text{eh}} = C'_1 \left\{ \frac{m_e^*}{m_h^*} + \frac{m_h^*}{m_e^*} \right\} + C'_2 - \frac{3B'C''}{C}.$$

The first contribution to this shift is nothing else but the sum of the contributions of the Stark shift undergone by the ground states of both electron and hole taken individually and computed by the variational principle formalism presented in Subsection 3.1. Because of the dependence of the constant  $\Gamma_{\text{var}}^{\text{eh}}$  on the effective masses  $m_{e,h}^*$ , let us remark that the second contribution to the Stark shift indicates the existence of a further physical coupling between electron and hole, which seems to be physically interpretable as a standard dipolar interaction between the two carriers of opposite electric charge. Actually, this interpretation is nothing more than a question of point view. Until now, we choose to consider that the interaction between the electron or the hole with the external electric field takes place individually, whereas the electron and the hole interact only through the Coulomb potential. This physical description justifies *a priori* the validity of the strong confinement regime assumption, for which the exciton states consist of uncorrelated individual confined electron and hole states, and then allows us to intuitively build a coherent and reasonable model in order to describe QCSE in QDs in this regime. Moreover, it also simplifies the calculations in practice. In spite of these advantageous properties, the previous remark suggests that we have to revise this picture. As a matter of fact, the electric field interaction part of the total Hamiltonian  $W_e(\mathbf{r}_e) + W_h(\mathbf{r}_h)$  should also be written as

$$W(\mathbf{r}_{\text{eh}}) = W_e(\mathbf{r}_e) + W_h(\mathbf{r}_h) = \mathbf{E}_d \cdot \mathbf{d}_{\text{eh}},$$

where  $\mathbf{d}_{\text{eh}} = e\mathbf{r}_{\text{eh}}$  is the exciton electric dipole moment, which is the standard dipolar interaction Hamiltonian of an electric dipole generated by two carriers, one with charge  $-e$  and another with charge  $+e$ . This dipolar interaction Hamiltonian satisfies the electron-hole exchange symmetry, while the individual interaction Hamiltonian  $W_{e,h}(\mathbf{r}_{e,h})$  transform themselves one into another. In the strong confinement regime, despite the importance of confinement effects on excitonic effects, the dipolar interaction point of view expresses the remnant of electron-hole pair states, thought as exciton bound states under the influence of the electric field. The dipolar interaction interpretation suggests the inclusion of a further term in the Hamiltonian  $H$  describing the exciton-electric field interaction, which accounts for the polarization energy of the electron-hole pair, due to the difference between the dielectric constants of the semiconductor QD and the surrounding insulating matrix.

Furthermore, we can explicitly confirm that another contribution to the confinement Hamiltonian  $H_0$  mean value, discarded because of the electron-hole exchange symmetry, does not effectively contribute to Stark effects. Using Eqs. (13), we obtain

$$\frac{K_h(\sigma, \sigma_e, \sigma_h)}{2m_h^* \langle \Phi | \Phi \rangle} - \frac{K_e(\sigma, \sigma_e, \sigma_h)}{2m_e^* \langle \Phi | \Phi \rangle} = \left\{ \frac{C'_1}{2} + \frac{C'_2}{4} \right\} \left\{ \frac{\sigma_h}{m_h^*} - \frac{\sigma_e}{m_e^*} \right\} \{\sigma_e + \sigma_h\} \sigma R + \dots$$

Thus, such terms contribute to the total Hamiltonian mean value  $H$  up to the third order in  $\frac{R}{a^*}$ . These third order terms just contribute to the variational parameters  $\sigma'_0$  and  $\sigma_{e,h}^0$  up to the first order, but not at all to the electron-hole pair ground state energy. Therefore, the last possible contribution to Stark effect should come from  $\left. \frac{K_h(\sigma, \sigma_e, \sigma_h)}{2m_h^* \langle \Phi | \Phi \rangle} - \frac{K_e(\sigma, \sigma_e, \sigma_h)}{2m_e^* \langle \Phi | \Phi \rangle} \right|_{\sigma'=\sigma'_0, \sigma_{e,h}=\sigma_{e,h}^0}$ , where we replace the different variational parameters by their respective zeroth order expressions, *i.e.*  $\sigma'_0 \approx 4B'$  and  $\sigma_{e,h}^0 \approx \frac{4C}{3} m_{e,h}^* e E_d R^2$ . Then, we straightforwardly have

$$\left. \frac{K_h(\sigma, \sigma_e, \sigma_h)}{2m_h^* \langle \Phi | \Phi \rangle} - \frac{K_e(\sigma, \sigma_e, \sigma_h)}{2m_e^* \langle \Phi | \Phi \rangle} \right|_{\sigma'=\sigma'_0, \sigma_{e,h}=\sigma_{e,h}^0} = 0,$$

which expresses what was expected.

### 3.4. Comparison with experimental data

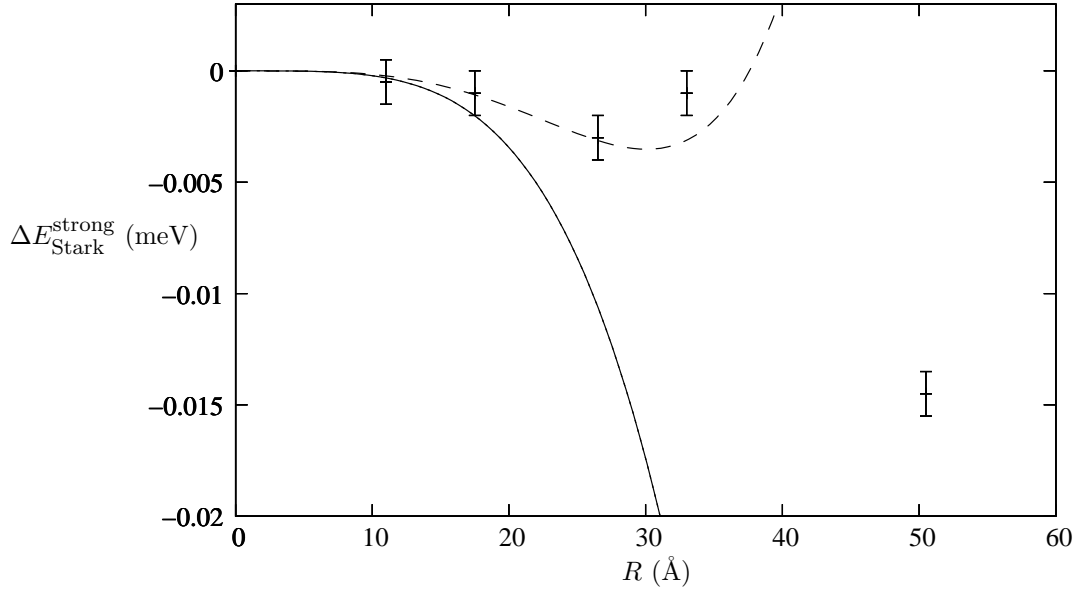
In order to test the relevance of our model, we shall compare numerical predictions we manage to compute to real experimental data [40] and to other computational data [41].

#### 3.4.1. Comparison with real experimental data

Figure 1 presents a comparison between results we obtain and experimental values for spherical  $CdS_{0.12}Se_{0.88}$  micro-crystallites [40]. The authors of [40] are able to experimentally resolve two exciton peaks, which they attribute to the transitions from the highest valence sub-band and from the spin-orbit split-off state to the lowest conduction sub-band. Furthermore, they observed that the energy splitting is about 0.39eV independently of the QD radius. The experimental values depicted by crosses in Figure 1 consist of the mean values of the Stark shift of these two types of excitons. They seem to indicate that the Coulomb interaction is sufficient to explain correctly the amplitude of the Stark effects experimentally observed, as we expect, in the range of validity of QD radii.

This paper offers a model, which is able to describe QCSE at least in the strong confinement regime for QD sizes  $R \leq \frac{2}{3\sigma'_0} a^*$ . But, we should remember that  $\sigma'_0$  is actually itself a function of  $\frac{R}{a^*}$ , which is still considered as a small dimensionless parameter in the strong confinement regime. Here, for convenience, we prefer to neglect the part of  $\sigma'_0$ , which depends on the electric field, because it scales as  $\propto m_e e^2 E_d^2 R^4$ . This is at least of the same order of magnitude as the exciton Rydberg energy as soon

**Figure 1.** Stark shift for confined interactive electron-hole pair as a function of the QD radius including the Coulomb interaction and excluding the polarization energy up to the zeroth (—) or to the first (---) order in comparison with experimental results (+) [40] in spherical  $CdS_{0.12}Se_{0.88}$  micro-crystallites with material parameters:  $\varepsilon = 9.3$ ,  $m_e^* = 0.13m_e$ ,  $m_h^* = 0.46m_e$ ,  $E^* = 16\text{meV}$  and  $a^* = 49\text{\AA}$ , where  $m_e$  is the electron bare mass. The electric field amplitude inside the micro-crystal is fixed at  $E_d = 12.5\text{kV.cm}^{-1}$  and  $\Gamma_{\text{var}}^{\text{eh}} \approx -0.1629$ .



as  $R \leq 50\text{\AA}$ , if the electric field amplitude is fixed at  $E_d = 12.5\text{kV.cm}^{-1}$ . We should also remark that  $\frac{CC''(m_e^* + m_h^*)}{12B'C'} \approx 0.0552m_e$ , hence

$$\begin{aligned} \sigma'_0 &= 4B' + 32B'C' \left\{ 1 - \frac{CC''}{12B'C'} (m_e^* + m_h^*) \frac{e^2 E_d^2 R^4}{E^*} \right\} \frac{R}{a^*} \\ &\approx 4B' \left\{ 1 + 8C' \frac{R}{a^*} \right\}. \end{aligned}$$

Therefore, up to the first order in  $\frac{R}{a^*}$ , our predictions should be valid for QD sizes with

$$R \leq \frac{a^*}{2(3B' + 4C')} \approx 0.6080a^*. \quad (18)$$

According to this effective constraint, in the case of  $CdS_{0.12}Se_{0.88}$  micro-crystals, this approach should lead to acceptable results in regard to experimental data as long as the cluster radius does not exceed  $30\text{\AA}$ . Figure 1 shows that the absolute value of the Stark shift, we compute up to the zeroth order, is significantly overestimated, except for a minor range of small QD radii compared with the one we expect. The results become much more accurate, if we carry the computation of the Stark effects up to the first order. In fact, in this case, Figure 1 also exhibits a good agreement with the experimental data over the whole expected region of micro-crystals radii. In this domain

of validity, the first order calculation seems to be efficient enough to describe QCSE in spherical semiconductor QDs. As soon as, the QD radius exceeds the maximal value for which the strong confinement regime is valid, our results diverge significantly from experimental data.

Finally, we have to determine the maximal electric field amplitude, for which the weak electric field limit assumption remains valid. To this end, as already previously explained, we must reconsider the consistency condition (9) for the electron or for the hole, in which we replace the respective variational parameters by their variational values. After summing the expressions for the electron and for the hole, up to the first order in  $\frac{R}{a^*}$ , we deduce, by also using the previous inequality which determines the strong confinement validity domain, that

$$\frac{E_{\text{ele}}}{E_{\text{eh}}} \leq \frac{6}{\pi^2 e} \frac{B' R}{C a^*} \leq \frac{1}{\pi^2 e C} \frac{1}{1 + \frac{4}{3} \frac{C'}{B'}} \approx 0.1197.$$

Then, in the strong confinement regime, the hypothesis of weak electric field limit should be valid as soon as the typical electric dipole interaction energy does not represent more than about 12% of the typical exciton confinement energy. Thus, if the micro-crystal radius is fixed at  $R = 10\text{\AA}$ , the highest electric field amplitude for which the weak field limit assumption stays acceptable is about  $E_{\text{d}}^{\text{max}} \approx 450\text{kV.cm}^{-1}$ , and *idem* if the QD radius is fixed near the upper boundary of the strong confinement regime validity domain, *i.e.*  $R \approx 30\text{\AA}$ , the electric field amplitude inside the QD should not exceed  $E_{\text{d}}^{\text{max}} \approx 16.7\text{kV.cm}^{-1}$ . These numerical results allow us to justify the fact that, taking an electric field such that  $E_{\text{d}}^{\text{max}} \approx 12.5\text{kV.cm}^{-1}$  to compare theoretical predictions against experimental results, satisfies the weak field limit all along the strong confinement range of valid QD radius.

In a more general manner, as soon as the semiconductor in the synthesized QD is chosen, the strong confinement regime domain of validity and the weak electric field limit condition consist of a set of two constraints, which should be optimized by choosing the QD radius and the electric field amplitude as functions of the Bohr radius, the Rydberg energy and the confinement energy of a trapped exciton. This is how we justify the validity of assumptions we made in order to use in practice the approach we propose in this article. But, for future technological applications, this set of constraints will permit to determine conversely the best possible semiconductor for practical and technological reasons, by imposing the typical QD size and the order of magnitude of the maximal electric field amplitude to use.

### 3.4.2. Comparison with computational data

In the early nineties, Nomura and Kobayashi performed a variational calculation on the same total Hamiltonian  $H$  with computational tools, in order to study Stark effect in spherical micro-crystals [41]. In their theoretical model, they also considered the weak field limit and expand the Hamiltonian mean value in powers of the variational parameters  $\sigma_{\text{e,h}}$ . However, they neglected terms, which scale as  $\propto \sigma_{\text{e,h}}^2$ , while they kept

**Table 1.** Stark shift for confined interactive electron-hole pair as a function of the QD radius including the Coulomb interaction and excluding the polarization energy, where terms scaling as  $\propto \sigma_{e,h}^2$  are removed from the total Hamiltonian  $H$  mean value, *i.e.*  $C'_1 = 0$  and  $\Gamma_{\text{var}}^{\text{eh}} \approx -0.0333$ , in comparison with computational results [41] in spherical  $\text{CdS}_{0.12}\text{Se}_{0.88}$  micro-crystallites.

R	Å	10	20	30	40	50
$-\Delta E_{\text{num}}$	meV	$2.08 \cdot 10^{-4}$	$3.16 \cdot 10^{-3}$	$1.49 \cdot 10^{-2}$	$4.34 \cdot 10^{-2}$	$9.63 \cdot 10^{-2}$
$-\Delta E_{\text{Stark}}^{\text{strong}}$	meV	$2.03 \cdot 10^{-4}$	$3.07 \cdot 10^{-3}$	$1.46 \cdot 10^{-2}$	$4.31 \cdot 10^{-2}$	$9.78 \cdot 10^{-2}$
relative error		<3%	<3%	$\approx 2\%$	<1%	<2%

terms scaling as  $\propto \sigma_e \sigma_h$ . Our approach suggests that such terms have the same order of magnitude and they both contribute to the electron-hole pair Stark shift. In fact, leaving out these contributions implies that  $C'_1$  should vanish in Eq. (14). Therefore, the expected Stark shift should be affected, because  $\Gamma_{\text{var}}^{\text{eh}}$  should be then expressed as  $\Gamma_{\text{var}}^{\text{eh}} = C'_2 - \frac{3B'C''}{C}$ . We first remark that  $\Gamma_{\text{var}}^{\text{eh}}$  is now independent of the semiconductor. Furthermore, we get  $\Gamma_{\text{var}}^{\text{eh}} \approx -0.0333$ , which hardly represents about 20% of its value, when we account for contributions scaling as  $\propto \sigma_{e,h}^2$ , *i.e.* if  $C'_1 \neq 0$ . The approximation made in [41] deeply changes the nature of Stark effect and does not seem to describe correctly experimental results, except for very small QDs.

However, Table 1 shows good agreement between our results for  $C'_1 = 0$  and computational ones from [41], even outside the validity domain of the strong confinement regime, *i.e.* for QD size  $R \geq 30\text{Å}$ . This signifies notably that, in the strong confinement regime, a first order expansion in  $\frac{R}{a^*}$  of the ground state energy Stark shift should be sufficient, at least when only the Coulomb interaction is included in the electron-hole pair Hamiltonian, because there is no particular constraint on the variational parameter  $\sigma$  in [41].

#### 4. Stark effects with polarization energy

In order to investigate in more details Stark effects in semiconductor micro-crystallites and to especially integrate, as a whole, the electric dipole interaction point of view, we shall introduce the following polarization energy employed by Brus in [8] to the total electron-hole Hamiltonian  $H$

$$P(\mathbf{r}_e, \mathbf{r}_h) = \frac{e^2}{2R} \sum_{l \geq 1} \alpha_l(\varepsilon_r) \left\{ \left( \frac{r_e}{R} \right)^{2l} + \left( \frac{r_h}{R} \right)^{2l} - 2 \left( \frac{r_e r_h}{R^2} \right)^l P_l(\cos \theta_{eh}) \right\},$$

where  $P_l(x)$  denotes the Legendre polynomial of index  $l$  and of variable  $x$ , and where we define, for a later purpose, the constants  $\alpha_l(\varepsilon_r)$  as functions of the relative dielectric constant  $\varepsilon_r$  as  $\alpha_l(\varepsilon_r) = \frac{l-1}{4\pi\varepsilon} \frac{\varepsilon_r - 1}{l\varepsilon_r + l + 1}$ ,  $l \in \mathbb{N}^*$ . We wish to apply once again the

variational method to the new total Hamiltonian  $H' = H + P$ , which takes into account the polarization energy  $P(\mathbf{r}_e, \mathbf{r}_h)$ . For this, we keep the form of the variational trial function  $\Phi(\mathbf{r}_e, \mathbf{r}_h)$ , since the polarization energy should not basically change the properties of the trial function.

#### 4.1. Stark effect in the strong confinement regime

Here, we are able to determine an expansion in the variational parameters of the mean value of the polarization energy, which presents the exact same form as the mean value of the Coulomb potential, where the constants  $A$ ,  $B'$ ,  $C'$ ,  $C'_1$  and  $C'_2$  are replaced by functions of the relative dielectric constant  $\varepsilon_r$ . This is the reason why we adopt the same notations for these quantities, but with explicit dependence on  $\varepsilon_r$ , as shown in Table B3. In fact, we can prove that the mean value of the polarization energy in the quantum state defined by  $\Phi(\mathbf{r}_e, \mathbf{r}_h)$  should be written as

$$\frac{\langle \Phi | P(\mathbf{r}_e, \mathbf{r}_h) | \Phi \rangle}{\langle \Phi | \Phi \rangle} = -\frac{e^2}{\kappa R} \left\{ A(\varepsilon_r) + B'(\varepsilon_r) \sigma R + C'(\varepsilon_r) \sigma^2 R^2 + C'_1(\varepsilon_r) (\sigma_e^2 + \sigma_h^2) R^2 + C'_2(\varepsilon_r) \sigma_e \sigma_h R^2 + O(\sigma^3 R^3) \right\}. \quad (19)$$

In this formalism, we obtain expressions for the variational parameters, the total electron-hole pair ground state energy and the Stark shift considering, on one hand, only the polarization energy or, on the other hand, both the Coulomb interaction and the polarization energy in Stark effects by Eqs. (15), (16) and (17) in Section 3, where we replace all the appearing constants, in the first case, by the corresponding functions of  $\varepsilon_r$  and, in the second case, by the sum of both contributions.

The most important step in the calculation consists of the simple idea of rewriting the functions  $\alpha_l(\varepsilon_r)$  in a such way that it becomes possible to perform analytically the summation of the series appearing in the expression of the Brus polarization energy. As matter of fact, we remark that for  $l \in \mathbb{N}^*$

$$\begin{aligned} \alpha_l(\varepsilon_r) &= \frac{\varepsilon_r - 1}{\kappa(\varepsilon_r + 1)} \left\{ 1 + \frac{\varepsilon_r}{(\varepsilon_r + 1)l + 1} \right\} \\ &\approx \frac{\varepsilon_r - 1}{\kappa(\varepsilon_r + 1)} \left\{ 1 + \frac{\varepsilon_r}{(\varepsilon_r + 1)l} \right\} = \tilde{\alpha}_l(\varepsilon_r). \end{aligned}$$

Let us introduce  $\Delta_l(\varepsilon_r)$  for  $l \in \mathbb{N}^*$ , as the relative error between the functions  $\alpha_l(\varepsilon_r)$  and  $\tilde{\alpha}_l(\varepsilon_r)$ . Therefore, the replacement of  $\alpha_l(\varepsilon_r)$  by  $\tilde{\alpha}_l(\varepsilon_r)$  is reasonable because it leads to negligible relative errors: *e.g.* for  $CdS_{0.12}Se_{0.88}$  micro-crystallites, for which  $\varepsilon_r = 4.0$ , we get that  $\Delta_1(\varepsilon_r) \approx 8\%$ ,  $\Delta_2(\varepsilon_r) \approx 3\%$  and  $\Delta_l(\varepsilon_r) = \frac{\varepsilon_r}{(\varepsilon_r + 1)^2} \frac{1}{l(l+1)} \lesssim 1\%$ , for  $l \geq 3$ .

The polarization energy is then written as

$$\begin{aligned} P(\mathbf{r}_e, \mathbf{r}_h) &= \frac{e^2}{2\kappa R} \frac{\varepsilon_r - 1}{\varepsilon_r + 1} \left[ \frac{1}{1 - \frac{r_e^2}{R^2}} + \frac{1}{1 - \frac{r_h^2}{R^2}} - \frac{\varepsilon_r}{\varepsilon_r + 1} \left\{ \log \left( 1 - \frac{r_e^2}{R^2} \right) + \log \left( 1 - \frac{r_h^2}{R^2} \right) \right\} \right. \\ &\quad \left. - 2 \sum_{l \geq 0} \left( \frac{r_e r_h}{R^2} \right)^l P_l(\cos \theta_{eh}) - \frac{2\varepsilon_r}{\varepsilon_r + 1} \sum_{l \geq 1} \frac{1}{l} \left( \frac{r_e r_h}{R^2} \right)^l P_l(\cos \theta_{eh}) \right], \quad (20) \end{aligned}$$

where it is possible to sum *a priori* the series in the polarization energy because of the confining potential well. In the mean value of  $P(\mathbf{r}_e, \mathbf{r}_h)$  in the quantum state  $\Phi(\mathbf{r}_e, \mathbf{r}_h)$ , only contribute the electron and hole coordinates such that  $r_{e,h} < R$ , *i.e.*  $\frac{r_{e,h}}{R}$  belongs to the convergence disc of the occurring series.

## 4.2. Comparison with experimental data

### 4.2.1. Comparison with real experimental data

We begin to evaluate the strong confinement regime validity region by considering Eq. (18), on which we apply the appropriate changes according to the cases. If we only consider the polarization energy, the strong confinement regime is not actually valid, because it turns out that  $\sigma'_0 \leq 0$ , in this case. Therefore, the interaction part of the variational function yields  $\phi_{\text{rel}}(r_{e,h}) = e^{|\sigma'_0|r_{e,h}}$ , this reveals the fact that the polarization energy is repulsive, while our approach is build on an attractive point of view for the interaction between the electron and the hole. If we consider both Coulomb potential and polarization energy, this problem no longer exists because the attractive effects of Coulomb potential are more important than the repulsive ones due to the polarization energy, so that  $\sigma'_0$  remains positive. Thus, the strong confinement regime remains valid up to  $R \lesssim 1.0179a^*$ , *i.e.*  $R \lesssim 49.9\text{\AA}$  for  $CdS_{0.12}Se_{0.88}$  micro-crystallites. This domain of validity is twice as large as the one obtained if only the Coulomb potential is taken into account.

In the same spirit, we can evaluate an order of magnitude for the maximal electric field amplitude, for which the limit of weak electric field should be assumed to be valid up to  $\frac{E_{\text{ele}}}{E_{\text{eh}}} \lesssim 0.1186$ , when only polarization is taken into account, and  $\frac{E_{\text{ele}}}{E_{\text{eh}}} \lesssim 0.1204$ , when polarization energy and Coulomb interaction are both included. From such numerical values, we should remark that the weak field limit is relatively insensitive to the interaction between the charge carriers. It may notably signify that this limit is relevantly chosen because it is an independent condition coming from the strong confinement regime validity domain. For example, this corresponds, for a QD radius of  $30\text{\AA}$ , to an electric field amplitude of about  $E_d = 16.5\text{kV.cm}^{-1}$ , on one hand, and to an electric field amplitude of about  $E_d = 16.8\text{kV.cm}^{-1}$ , on the other hand.

As the electric field amplitude is fixed inside the  $CdS_{0.12}Se_{0.88}$  micro-crystallites at  $E_d = 12.5\text{kV.cm}^{-1}$ , the weak electric field limit should be satisfied in the range of QD radii  $R \leq 30\text{\AA}$  and we can compare, at least in this domain, our predictions to experimental data. In the rest of the strong confinement regime validity domain, *i.e.* for radii  $30\text{\AA} \lesssim R \lesssim 50\text{\AA}$ , the weak field limit is no longer valid. This may actually explain the significant divergence from experimental results in this region. Once again the analogy with rectangular quantum boxes should be quite helpful. In the opposite limit of strong electric field, the Stark shift undergone by the ground state of the electron-hole pair confined in a rectangular QD shows essentially a linear behavior in the electric field amplitude [34], which is a totally different behavior in comparison with the quadratic dependence found here.



**Figure 2.** Stark shift for confined interactive electron-hole pair as a function of the QD radius including the both Coulomb interaction and polarization energy up to the zeroth (—) or to the first order (---), where  $\Gamma_{\text{var}}^{\text{eh}} \approx -0.2045$ , and including only the polarization energy up to the first order (-·-), where  $\Gamma_{\text{var}}^{\text{eh}} \approx -0.0416$ , in comparison with experimental results (+) [40] in spherical  $\text{CdS}_{0.12}\text{Se}_{0.88}$  micro-crystallites with material parameters. The electric field amplitude inside the micro-crystal is once again fixed at  $E_d = 12.5 \text{ kV.cm}^{-1}$ .

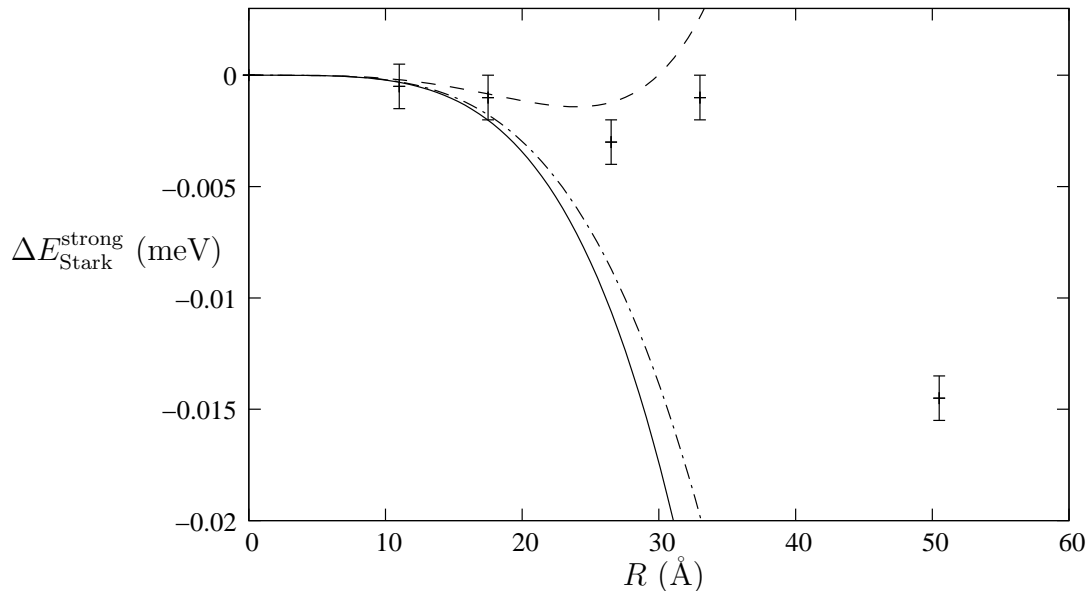


Figure 2 also clearly shows that the behavior of the polarization energy, if considered alone, is not satisfactory because it seems that its contribution does not counterbalance the divergence of the zeroth order Stark shift for QD radii near the upper boundary of the strong confinement validity region, while Figure 1 suggests that the contribution to the Stark effects due to the Coulomb potential seems to consist of more important contributions. Figure 2 stresses this point of view because, in the strong confinement regime, the results we obtain, if we account for the Coulomb potential and the polarization energy accurately, fit the experimental data, except if the QD size begins to reach the upper boundary of the validity domain of this regime, when only the Coulomb potential is included, and the weak field limit is not valid anymore. The reason for this phenomenon is simple to understand. For such QD sizes, we can easily show that the first order term actually has the same order of magnitude as the zeroth order contribution to the Stark shift. Then, if it is reasonable to maintain *a priori* a perturbation point of view, the first order correction is not sufficient to describe correctly QCSE in the whole domain of strong confinement regime validity. It is perhaps advisable to continue the expansion to one or two further orders and to revise the definition of weak field limit. However, the computations become quite involved and we think that such approach does not really bring a significant improvement to the understanding of the Stark effects in QDs.

**Table 2.** Stark shift for confined interactive electron-hole pair as a function of the QD radius including the Coulomb interaction and the polarization energy where terms scaling as  $\propto \sigma_{e,h}^2$  are suppressed from the total Hamiltonian  $H$  mean value, *i.e.*  $C'_1(\varepsilon_r), C'_1 = 0$  and  $\Gamma_{\text{var}}^{\text{eh}} \approx -0.0446$ , in comparison with computational results [41] in spherical  $\text{CdS}_{0.12}\text{Se}_{0.88}$  micro-crystallites.

R	Å	10	20	30	40	50
$-\Delta E_{\text{num}}$	meV	$2.09 \cdot 10^{-4}$	$3.14 \cdot 10^{-3}$	$1.45 \cdot 10^{-2}$	$4.11 \cdot 10^{-2}$	$8.93 \cdot 10^{-2}$
$-\Delta E_{\text{Stark}}^{\text{strong}}$	meV	$1.99 \cdot 10^{-4}$	$2.94 \cdot 10^{-3}$	$1.36 \cdot 10^{-2}$	$3.90 \cdot 10^{-2}$	$8.55 \cdot 10^{-2}$
relative error		$\approx 5\%$	$\approx 6\%$	$\approx 6\%$	$\approx 5\%$	$\approx 4\%$

#### 4.2.2. Comparison with computational data

Following the reasonings and remarks we made in Subsubsection 3.4.2, we add the polarization energy  $P(\mathbf{r}_e, \mathbf{r}_h)$  to the total Hamiltonian of the electron-hole pair but impose that  $C'_1(\varepsilon_r), C'_1 = 0$ , in such a way that terms scaling as  $\propto \sigma_{e,h}^2$  do not contribute to the electron-hole ground state Stark shift. Once again, the new value for  $\Gamma_{\text{var}}^{\text{eh}}$  represents a small part from the one, in which all contributions are kept. Likewise, when we only consider the Coulomb interaction, Table 2 shows that there is still a good agreement between our results and computational ones from [41], over the whole validity domain of strong confinement regime. The divergence from experimental results is still significant after including the polarization energy, even for small QD radius. This confirms that the terms scaling  $\propto \sigma_{e,h}^2$  play a relevant role in Stark effects and should not be discarded. While, this also legitimates the approximation  $\alpha_l(\varepsilon_r) \approx \tilde{\alpha}_l(\varepsilon_r)$ , because Table 2 suggests that this approximation does not seem over-estimate the polarization energy contribution to the Stark shift. Maybe, each term of the sum defining the polarization energy plays a role in Stark effect, but errors made term by term should not cumulate.

A first order expansion in  $\frac{R}{a^*}$  of the ground state energy Stark shift should not be sufficient and reinforces the idea according which it is necessary to carry on the expansion at least up to the second order. If the second order expansion does not improve the situation, this signifies that there should exist another reason for this divergence. Therefore, because the strong confinement regime validity domain is not affected by dropping of terms scaling  $\propto \sigma_{e,h}^2$ , it is reasonable to think that it comes from the failure of the weak field limit assumption for QD radius sufficiently close to its upper boundary.

## 5. Conclusion

By considering a simple EMA-model under the assumptions of strong confinement regime by a infinite potential well and of weak electric field limit, we are able to obtain analytical results for Stark effect in semiconducting micro-crystallites with spherical

shape. In the domain of validity of physical approximations, the numerical values we can deduce agree with experimental data. We furthermore clarify why other variational calculations predict numerical results, which markedly diverge from experimental ones.

Despite these successes, our approach has been invalidated in a particular range of QD sizes, for which the strong confinement point of view still holds, but for which the weak electric field limit assumption fails. Thus, a future research work may focus on trying to apply the strong confinement regime in the limit of strong electric field indeed, or even in a more general manner, to any electric field amplitude. The case of the weak confinement regime of the electron-hole pair is much more difficult, even in the weak field limit. Actually, in such a regime, the integration domain of integrals, we have to deal with, to compute the square of the trial function norm or the diagonal matrix elements of physical operators consists of a half-rectangle instead of the domain  $\mathcal{D}$ , which is a half-square. This implies an explicit break down of the electron-hole exchange symmetry. Then, a different approach may be needed.

## Appendix A. Calculations of norms

As suggested by the remark on translation invariance and spherical symmetry breakdown as a whole in Subsubsection 2.3.1, the square of the norms of the trial functions  $\phi(\mathbf{r}_e, \mathbf{r}_h)$  and  $\Phi(\mathbf{r}_e, \mathbf{r}_h)$  should be computed by using Fourier transform formalism in relative coordinates. Then, let  $\mathcal{F}[f]$  stands for the Fourier transform of a function  $f$ . In order to prove the derivation of Eqs. (4) and (8), we need the expressions of the Fourier transform of the functions  $\psi_{010}^2$  and  $\phi_{\text{rel}}^2$ . It can be shown straightforwardly that

$$\begin{cases} \mathcal{F}[\phi_{\text{rel}}^2](\mathbf{k}) &= -4\pi\partial_\sigma \frac{1}{\sigma^2 + k^2}, \\ \mathcal{F}[\psi_{010}^2](\mathbf{k}) &= \frac{2}{kR} \int_0^1 \frac{dx}{x} \sin^2(\pi x) \sin(kRx). \end{cases}$$

### Appendix A.1. State norm in absence of electric field

As  $\phi_{\text{rel}}^2, \mathcal{F}[\phi_{\text{rel}}^2] \in L^1(\mathbb{R}^3)$ , the inversion theorem of the Fourier transform is satisfied and yields

$$\phi_{\text{rel}}^2(\mathbf{r}) = \int_{\mathbb{R}^3} \frac{d^3\mathbf{k}}{(2\pi)^3} \mathcal{F}[\phi_{\text{rel}}^2](\mathbf{k}) e^{i\mathbf{k}\cdot\mathbf{r}}, \quad \forall \mathbf{r} \in \mathbb{R}^3.$$

Then,

$$\begin{aligned} \langle \phi | \phi \rangle &= \int_{(\mathbb{R}^3)^2} d^3\mathbf{r}_e d^3\mathbf{r}_h \psi_{010}^2(\mathbf{r}_e) \psi_{010}^2(\mathbf{r}_h) \phi_{\text{rel}}^2(\mathbf{r}_{eh}) \\ &= \int_{\mathbb{R}^3} \frac{d^3\mathbf{k}}{(2\pi)^3} \mathcal{F}[\phi_{\text{rel}}^2](\mathbf{k}) \mathcal{F}[\psi_{010}^2](\mathbf{k})^2 \\ &= -\frac{8}{\pi R^2} \partial_\sigma \iint_{[0,1]^2} \frac{dx}{x} \frac{dy}{y} \sin^2(\pi x) \sin^2(\pi y) \int_0^\infty \frac{dk}{\sigma^2 + k^2} \sin(kRx) \sin(kRy). \end{aligned}$$

Since, according to Eq. **2.5.6.4**, p. 390 [55], we get

$$\int_0^\infty \frac{dk}{\sigma^2 + k^2} \sin(kRx) \sin(kRy) = \frac{\pi}{4\sigma} \{e^{-\sigma R|x-y|} - e^{-\sigma R(x+y)}\}, \quad \forall (x, y) \in [0, 1]^2.$$

Therefore, the expression for  $\langle \phi | \phi \rangle$ , after some trivial manipulations, becomes

$$\langle \phi | \phi \rangle = -\frac{8}{R^2} \partial_\sigma \frac{1}{\sigma} \iint_{\mathcal{D}} \frac{dx}{x} \frac{dy}{y} \sin^2(\pi x) \sin^2(\pi y) \sinh(\sigma Rx) e^{-\sigma Ry}.$$

The corresponding expression for the Coulomb potential diagonal element  $\langle \phi | V_C | \phi \rangle$  should be obtained in the same way, up to the homogeneity factor, except that  $\phi_{\text{rel}}^2(r_{\text{eh}})$  should be replaced by  $\varphi_{\text{rel}}(r_{\text{eh}}) = -\frac{e^2}{\kappa} \frac{\phi_{\text{rel}}(r_{\text{eh}})^2}{r_{\text{eh}}}$ , where  $\mathcal{F}[\varphi_{\text{rel}}](\mathbf{k}) = -\frac{e^2}{\kappa} \frac{4\pi}{\sigma^2 + k^2}$ .

### Appendix A.2. State norm in presence of electric field

Here, we argue as in the previous subsection, except that we have to pay attention to the fact that the Fourier transform of the electronic and hole trial function parts are no longer identical, *i.e.* we should write, because  $\langle \Phi | \Phi \rangle \in \mathbb{R}$ ,

$$\langle \Phi | \Phi \rangle = \int_{\mathbb{R}^3} \frac{d^3\mathbf{k}}{(2\pi)^3} \mathcal{F}[\phi_{\text{rel}}^2](\mathbf{k}) \mathcal{F}[\varphi_e^2 \psi_{010}^2](\mathbf{k}) \overline{\mathcal{F}[\varphi_h^2 \psi_{010}^2](\mathbf{k})}.$$

Later on, in spherical coordinates, we shall adopt the following notations

$$\mathbf{r} = \begin{pmatrix} r \sin \theta \cos \varphi \\ r \sin \theta \sin \varphi \\ r \cos \theta \end{pmatrix} \quad \text{and} \quad \mathbf{k} = \begin{pmatrix} k \sin \theta' \cos \varphi' \\ k \sin \theta' \sin \varphi' \\ k \cos \theta' \end{pmatrix},$$

where  $r, k \geq 0$ ;  $\theta, \theta' \in [0, \pi]$  and  $\varphi, \varphi' \in [0, 2\pi]$ .

#### Appendix A.2.1. Calculation of $\mathcal{F}[\varphi_{e,h}^2 \psi_{010}^2]$

It is easy to show that

$$\begin{aligned} & \mathcal{F}[\varphi_{e,h}^2 \psi_{010}^2](\mathbf{k}) \\ &= \frac{1}{2\pi R} \int_0^R dr \sin^2\left(\frac{\pi}{R}r\right) \int_0^\pi d\theta \sin \theta e^{\pm \sigma_{e,h} r \cos \theta} e^{ikr \cos \theta \cos \theta'} \int_0^{2\pi} d\varphi e^{-ikr \sin \theta \sin \theta' \cos(\varphi - \varphi')}. \end{aligned}$$

Since, according to Eq. **8.411.1**, p. 902 [57], we have, first

$$\begin{aligned} \int_0^{2\pi} d\varphi e^{-ikr \sin \theta \sin \theta' \cos(\varphi - \varphi')} &= \int_{-\pi}^{\pi} d\varphi e^{-ikr \sin \theta \sin \theta' \sin \varphi} \\ &= 2\pi J_0(kr \sin \theta \sin \theta'). \end{aligned}$$

Second, according to Eq. **5.13.3.8**, p. 713 [56],

$$e^{iz \cos \alpha \cos \beta} J_0(z \sin \alpha \sin \beta) = \sqrt{\frac{2\pi}{kr}} \sum_{n \geq 0} i^n \left(n + \frac{1}{2}\right) J_{n+\frac{1}{2}}(z) C_n^{\frac{1}{2}}(\cos \alpha) C_n^{\frac{1}{2}}(\cos \beta),$$

where  $C_n^\lambda(x)$  is the Gegenbauer polynomial of indexes  $n$  and  $\lambda$  and of variable  $x$ . And, third, according to Eq. **2.21.5.1**, p. 527 [56], we have the integral representation

$$\int_{-1}^1 d\xi e^{-(\mp\sigma_{e,h}r)\xi} C_n^{\frac{1}{2}}(\xi) = (\pm 1)^n \sqrt{\frac{2\pi}{\sigma_{e,h}r}} I_{n+\frac{1}{2}}(\sigma_{e,h}r),$$

where  $I_\nu(x)$  is the modified Bessel function of the first kind of index  $\nu$  and variable  $x$ . We straightforwardly deduce that

$$\begin{aligned} & \int_0^\pi d\theta \sin \theta e^{\pm\sigma_{e,h}r \cos \theta} e^{ikr \cos \theta \cos \theta'} \int_0^{2\pi} d\varphi e^{-ikr \sin \theta \sin \theta' \cos(\varphi-\varphi')} \\ &= 2\pi \int_0^\pi d\theta \sin \theta e^{\pm\sigma_{e,h}r \cos \theta} e^{ikr \cos \theta \cos \theta'} J_0(kr \sin \theta \sin \theta') \\ &= 2\pi \sqrt{\frac{2\pi}{kr}} \sum_{n \geq 0} i^n \left(n + \frac{1}{2}\right) J_{n+\frac{1}{2}}(kr) C_n^{\frac{1}{2}}(\cos \theta') \int_{-1}^1 d\xi e^{\pm\sigma_{e,h}r \xi} C_n^{\frac{1}{2}}(\xi) \\ &= \frac{4\pi^2}{r} \sqrt{\frac{1}{\sigma_{e,h}k}} \sum_{n \geq 0} (\pm i)^n \left(n + \frac{1}{2}\right) J_{n+\frac{1}{2}}(kr) I_{n+\frac{1}{2}}(\sigma_{e,h}r) C_n^{\frac{1}{2}}(\cos \theta'). \end{aligned}$$

Therefore, after some trivial manipulations, we obtain

$$\begin{aligned} & \mathcal{F}[\varphi_{e,h}^2 \psi_{010}^2](\mathbf{k}) \\ &= \frac{2\pi}{R} \sqrt{\frac{1}{\sigma_{e,h}k}} \sum_{n \geq 0} (\pm i)^n \left(n + \frac{1}{2}\right) C_n^{\frac{1}{2}}(\cos \theta') \int_0^1 \frac{dx}{x} \sin^2(\pi x) J_{n+\frac{1}{2}}(kRx) I_{n+\frac{1}{2}}(\sigma_{e,h}Rx). \end{aligned}$$

#### Appendix A.2.2. Calculation of $\langle \Phi | \Phi \rangle$

We put the value of  $\mathcal{F}[\varphi_{e,h}^2 \psi_{010}^2](\mathbf{k})$  in the previous expression for  $\langle \Phi | \Phi \rangle$  and obtain

$$\begin{aligned} & \langle \Phi | \Phi \rangle \\ &= \frac{-4\pi}{R^2 \sqrt{\sigma_e \sigma_h}} \partial_\sigma \int_0^1 \int_0^1 \frac{dx}{x} \frac{dy}{y} \sin^2(\pi x) \sin^2(\pi y) \sum_{n \geq 0} (-1)^n \left(n + \frac{1}{2}\right) I_{n+\frac{1}{2}}(\sigma_e Rx) I_{n+\frac{1}{2}}(\sigma_h Ry) \\ & \quad \int_0^\infty \frac{dk}{\sigma^2 + k^2} k J_{n+\frac{1}{2}}(kRx) J_{n+\frac{1}{2}}(kRy), \end{aligned}$$

after performing the integral over  $\theta'$ , using the Gegenbauer polynomials orthonogality (*c.f.* Eq. **2.21.18.10**, p. 563 [56]). Furthermore, if  $0 \leq x < y \leq 1$ , the integral over  $k$  should be evaluated, according to Eq. **2.12.32.11** p. 213 [56], as

$$\int_0^\infty \frac{dk}{\sigma^2 + k^2} k J_{n+\frac{1}{2}}(kRx) J_{n+\frac{1}{2}}(kRy) = I_{n+\frac{1}{2}}(\sigma Rx) K_{n+\frac{1}{2}}(\sigma Ry).$$

At this point, the last remaining problem consists in getting a compact expression for

$$\sum_{n \geq 0} (-1)^n \left(n + \frac{1}{2}\right) I_{n+\frac{1}{2}}(\sigma_{e,h}Rx) I_{n+\frac{1}{2}}(\sigma Rx) I_{n+\frac{1}{2}}(\sigma_{h,e}Ry) K_{n+\frac{1}{2}}(\sigma Ry),$$

where  $0 \leq x < y \leq 1$ .

To this end, we find an advantageous integral representation for the product of modified Bessel functions  $I_{n+\frac{1}{2}}(\sigma_{e,h}Ry)K_{n+\frac{1}{2}}(\sigma Ry)$ . In fact, in the weak field limit we should have  $\sigma_{e,h} < \sigma$ . Therefore, Eq. **3.8.2**, p. 90 [58] is applicable and we can write

$$I_{n+\frac{1}{2}}(\sigma_{e,h}Ry)K_{n+\frac{1}{2}}(\sigma Ry) = \frac{1}{2} \sqrt{\frac{\sigma_h}{\sigma}} \int_{-1}^1 d\xi C_n^{\frac{1}{2}}(\xi) \frac{e^{-\rho_{e,h}(\xi)\sigma Ry}}{\rho_{e,h}(\xi)}.$$

Moreover, under the validity of the consistency condition (9), according to Eq. **5.13.3.6**, p. 713 [56], in the case of the modified Bessel functions of the first kind, we deduce that

$$\sum_{n \geq 0} (-1)^n \left( n + \frac{1}{2} \right) I_{n+\frac{1}{2}}(\sigma_{e,h}Rx) I_{n+\frac{1}{2}}(\sigma Rx) C_n^{\frac{1}{2}}(\xi) = \frac{1}{\pi} \sqrt{\frac{\sigma_{e,h}}{\sigma}} \frac{\sinh(\rho_{e,h}(\xi)\sigma Rx)}{\rho_e(\xi)}.$$

Then, by grouping together the last two expressions, we obtain the result we have expected

$$\begin{aligned} & \sum_{n \geq 0} (-1)^n \left( n + \frac{1}{2} \right) I_{n+\frac{1}{2}}(\sigma_{e,h}Rx) I_{n+\frac{1}{2}}(\sigma Rx) I_{n+\frac{1}{2}}(\sigma_{h,e}Ry) K_{n+\frac{1}{2}}(\sigma Ry) \\ &= \frac{\sqrt{\sigma_e \sigma_h}}{2\pi\sigma} \int_{-1}^1 d\xi \frac{\sinh(\rho_{e,h}(\xi)\sigma Ry)}{\rho_{e,h}(\xi)} \frac{e^{-\rho_{h,e}(\xi)\sigma Ry}}{\rho_{h,e}(\xi)}. \end{aligned}$$

It finally shows that  $\langle \Phi | \Phi \rangle$  satisfies Eq. (8). And, if  $\frac{\sigma_{e,h}}{\sigma} \rightarrow 0$ , we observe that

$$\langle \Phi | \Phi \rangle \rightarrow \langle \phi | \phi \rangle.$$

## Appendix B. Constants

In the following tables, we sum up all appearing constants and give their approximate values, where the function  $\text{Si}(x)$  denotes the sine integral

$$\text{Si}(x) = \int_0^x \frac{dt}{t} \sin(t).$$

### Appendix B.1. Constants occurring in Stark effect expressions without polarization energy

Table B1 presents constants analytical expressions and approximate values when we only include the Coulomb potential.

### Appendix B.2. Constants occurring in Stark effect expressions with polarization energy

We evaluate the polarization energy mean value using Eq. (20). To this end, we compute integral representations of the polarization energy terms depending only on the radial coordinates  $r_{e,h}$  of the electron and the hole following the reasoning, made in Subsection 3.2 in order to get Eq. (8). This reasoning does not apply to the angular part. However, we are able to provide exact expressions for all the constants which appear in the calculations, except for  $\delta'''$ ,  $\gamma'''$  and  $\gamma''''$ . For these, we obtain integral representations,

**Table B1.** Definition, analytical expression and approximate value of constants when only the Coulomb interaction is taken into account.

Name	Expression	Value
$A$	$2 - \frac{1}{\pi} \left\{ \text{Si}(2\pi) - \frac{\text{Si}(4\pi)}{2} \right\}$	1.7861
$B_1$	$\frac{2}{3} - \frac{5}{8\pi^2}$	0.6033
$B_2$	$\frac{2}{9} + \frac{13}{24\pi^2} + \frac{1}{2\pi^3} \left\{ \text{Si}(2\pi) - \frac{\text{Si}(4\pi)}{2} \right\}$	0.2879
$B$	$B_1 + \frac{B_2}{3}$	0.6993
$B'$	$AB - 1$	0.2489
$C$	$\frac{1}{3} - \frac{1}{2\pi^2}$	0.2827
$C'$	$A(B^2 - C) - \frac{B}{2}$	0.0189
$C'_1$	$\frac{B_1 - 2AC}{12}$	-0.0339
$C'_2$	$\frac{B_2}{18}$	0.0160
$D_1$	$\frac{2}{5} - \frac{13}{8\pi^2} + \frac{147}{64\pi^4}$	0.2589
$D_2$	$\frac{2}{15} - \frac{1}{8\pi^2} - \frac{21}{64\pi^4}$	0.1173
$D_3$	$\frac{2}{25} + \frac{37}{120\pi^2} - \frac{1153}{320\pi^4} - \frac{3}{2\pi^5} \left\{ \text{Si}(2\pi) - \frac{\text{Si}(4\pi)}{2} \right\}$	0.0710
$D$	$\frac{5D_1 + 10D_2 + D_3}{30}$	0.2539
$D'$	$\frac{3D_1 + 4D_2 + D_3}{6}$	0.2195
$D''$	$\frac{5D_2 - D_3}{45}$	0.0115
$C''$	$\frac{D' + 3D'' - BC}{3}$	0.0187

which cannot be analytically computed at the moment. Their approximative values are then computed numerically by using Wolfram Research Mathematica<sup>®</sup> 7. Moreover, as exact expressions for other constants are quite cumbersome, we give their approximate values.

Let us define the constants  $\beta'$ ,  $\beta''$ ,  $\gamma'$ ,  $\gamma''$ ,  $\gamma'''$ ,  $\gamma''''$ ,  $\delta'$ ,  $\delta''$  and  $\delta'''$  by the expressions

$$\begin{aligned}
 & \langle \Phi | \frac{1}{1 - \frac{r_e^2}{R^2}} + \frac{1}{1 - \frac{r_h^2}{R^2}} | \Phi \rangle \\
 = & -\frac{2}{R^2} \partial_\sigma \int_{-1}^1 d\xi \iint_{\mathcal{D}} \frac{dx}{x} \frac{dy}{y} \sin^2(\pi x) \sin^2(\pi y) \left\{ \frac{1}{1-x^2} + \frac{1}{1-y^2} \right\} \\
 & \times \left\{ \frac{\sinh(\rho_e(\xi)\sigma Rx) e^{-\rho_h(\xi)\sigma Ry}}{\rho_e(\xi)} + \frac{\sinh(\rho_h(\xi)\sigma Rx) e^{-\rho_e(\xi)\sigma Ry}}{\rho_h(\xi)} \right\} \\
 = & \beta' - \gamma' \sigma R + \delta' \sigma^2 R^2 + \frac{\delta'}{6} (\sigma_e^2 + \sigma_h^2) R^2 + O(\sigma^3 R^3), \\
 & - \langle \Phi | \log\left(1 - \frac{r_e^2}{R^2}\right) + \log\left(1 - \frac{r_h^2}{R^2}\right) | \Phi \rangle \\
 = & -\frac{2}{R^2} \partial_\sigma \int_{-1}^1 d\xi \iint_{\mathcal{D}} \frac{dx}{x} \frac{dy}{y} \sin^2(\pi x) \sin^2(\pi y) \{ \log(1-x^2) + \log(1-y^2) \} \\
 & \times \left\{ \frac{\sinh(\rho_e(\xi)\sigma Rx) e^{-\rho_h(\xi)\sigma Ry}}{\rho_e(\xi)} + \frac{\sinh(\rho_h(\xi)\sigma Rx) e^{-\rho_e(\xi)\sigma Ry}}{\rho_h(\xi)} \right\} \\
 = & \beta'' - \gamma'' \sigma R + \delta'' \sigma^2 R^2 + \frac{\delta''}{6} (\sigma_e^2 + \sigma_h^2) R^2 + O(\sigma^3 R^3), \\
 & 2 \langle \Phi | \sum_{l \geq 0} \left( \frac{r_e r_h}{R^2} \right)^l P_l(\cos \theta_{eh}) | \Phi \rangle \\
 = & 2 - \gamma''' \sigma R - \delta''' \sigma^2 R^2 + 2C \left\{ \sigma^2 \frac{\sigma_e^2 + \sigma_h^2}{6} \right\} R^2 - \frac{\sigma_e \sigma_h}{18} R^2 + O(\sigma^3 R^3), \\
 & 2 \langle \Phi | \sum_{l \geq 1} \frac{1}{l} \left( \frac{r_e r_h}{R^2} \right)^l P_l(\cos \theta_{eh}) | \Phi \rangle \\
 = & -\gamma'''' \sigma R - \delta'''' \sigma^2 R^2 - \frac{\sigma_e \sigma_h}{18} R^2 + O(\sigma^3 R^3).
 \end{aligned}$$

Table B2 presents approximate values for constants which appear in the polarization energy diagonal matrix element  $\langle \Phi | P(\mathbf{r}_e, \mathbf{r}_h) | \Phi \rangle$ , while Table B3 defines constants which appear in the polarization mean value Eq. (19) and gives their approximate values in  $CdS_{0.12}Se_{0.88}$  micro-crystals.

### Appendix C. Matrix elements $\langle \psi_{lnm} | \mathbf{r} \cos \theta | \psi_{010} \rangle$

Let  $l, l' \in \mathbb{N}$ ;  $n, n' \in \mathbb{N}^*$  and  $m, m' \in \llbracket -l, l \rrbracket \times \llbracket -l', l' \rrbracket$ . Here, we present the general computation of the matrix element

$$\langle \psi_{lnm} | r \cos \theta | \psi_{l'n'm'} \rangle = 4R I_{nn'}^{ll'} J_{ll'}^{mm'},$$



**Table B2.** Approximate value of constants appearing in  $\langle \Phi | P(\mathbf{r}_e, \mathbf{r}_h) | \Phi \rangle$ .

Name	Value	Name	Value
$\beta'$	3.1144	$\beta''$	0.7524
$\gamma'$	2.3218	$\gamma''$	0.5992
$\delta'$	0.9973	$\delta''$	0.2708
$\gamma'''$	1.3263	$\gamma''''$	-0.0704
$\delta'''$	0.0533		

**Table B3.** Definition and approximate value of constants appearing in the polarization mean value Eq. (19) in  $CdS_{0.12}Se_{0.88}$  micro-crystals.

Name	Expression	Value for $CdS_{0.12}Se_{0.88}$
$\beta(\varepsilon_r)$	$\frac{1}{2} \frac{\varepsilon_r - 1}{\varepsilon_r + 1} \left\{ \beta' - 2 + \frac{\varepsilon_r}{\varepsilon_r + 1} \beta'' \right\}$	0.5149
$\gamma(\varepsilon_r)$	$\frac{1}{2} \frac{\varepsilon_r - 1}{\varepsilon_r + 1} \left\{ \gamma' - \gamma''' + \frac{\varepsilon_r}{\varepsilon_r + 1} (\gamma'' - \gamma'''' ) \right\}$	0.4594
$\delta_1(\varepsilon_r)$	$\frac{\varepsilon_r - 1}{\varepsilon_r + 1} \left\{ \delta' - 2C + \frac{\varepsilon_r}{\varepsilon_r + 1} \delta'' \right\}$	0.3891
$\delta_2(\varepsilon_r)$	$\frac{\varepsilon_r - 1}{2} \frac{2\varepsilon_r + 1}{(\varepsilon_r + 1)^2}$	0.5400
$\delta(\varepsilon_r)$	$\frac{\varepsilon_r - 1}{\varepsilon_r + 1} \left\{ \delta' + \delta''' - 2C + \frac{\varepsilon_r}{\varepsilon_r + 1} (\delta'' + \delta'''' ) \right\}$	0.4467
$A(\varepsilon_r)$	$-\beta(\varepsilon_r)$	-0.4467
$B'(\varepsilon_r)$	$-\beta(\varepsilon_r)B + \gamma(\varepsilon_r)$	-0.0993
$C'(\varepsilon_r)$	$-\beta(\varepsilon_r)(B^2 - C) + \gamma(\varepsilon_r)B - \frac{\delta(\varepsilon_r)}{2}$	-0.0083
$C'_1(\varepsilon_r)$	$-\frac{\delta_1(\varepsilon_r) - 2\beta(\varepsilon_r)C}{12}$	-0.0082
$C'_2(\varepsilon_r)$	$-\frac{\delta_2(\varepsilon_r)}{18}$	-0.0300

where we respectively introduce radial and angular integrals as

$$\begin{cases} I_{nn'}^{ll'} &= \int_0^1 dx x^2 J_{\nu_{l'}}(k_{l'n'}x) J_{\nu_l}(k_{ln}x), \\ J_{ll'}^{mm'} &= \int_0^{2\pi} \int_0^\pi \sin\theta d\theta d\varphi \overline{Y_{l'}^{m'}(\theta, \varphi)} \cos\theta Y_l^m(\theta, \varphi). \end{cases}$$

The basic idea to determine the angular integrals  $J_{ll'}^{mm'}$  consists in determining the angular function  $\cos\theta Y_l^m(\theta, \varphi)$  coordinates in the spherical harmonic functions basis applying by angular momentum theory. This calculation is treated in [54] and it is proved that

$$\cos\theta Y_l^m(\theta, \varphi) = \sqrt{\frac{(l+m+1)(l-m+1)}{(2l+3)(2l+1)}} Y_{l+1}^m(\theta, \varphi) + \sqrt{\frac{(l+m)(l-m)}{(2l+1)(2l-1)}} Y_{l-1}^m(\theta, \varphi).$$

Then, after integrating through the angles  $\theta$  and  $\phi$  by using the spherical harmonic functions orthonormal relations, we deduce that

$$J_{ll'}^{mm'} = \sqrt{\frac{(l+m)(l-m)}{(2l+1)(2l-1)}} \delta_{l'l-1} \delta^{m'm} + \sqrt{\frac{(l+m+1)(l-m+1)}{(2l+3)(2l+1)}} \delta_{l'l+1} \delta^{m'm}.$$

As angular integrals vanish if and only if  $l' \neq l \pm 1$  and  $m \neq m'$ , we should focus only on radial integrals of type  $I_{nn'}^{ll \pm 1}$ . Furthermore, we should recall the standard recurrence relation of Bessel functions of different indices,  $\forall z \in \mathbb{C}$  and  $\forall \nu > 0$

$$J_{\nu \pm 1}(z) = \frac{\nu}{z} J_\nu(z) \mp J'_\nu(z).$$

Thus, we can write

$$\begin{aligned} I_{nn'}^{ll \pm 1} &= \frac{1}{2J'_{\nu_l}(k_{ln})J'_{\nu_{l \pm 1}}(k_{l \pm 1n'})} \int_0^1 dx x J_{\nu_l}(k_{ln}x) \left\{ \frac{\nu_l}{k_{l \pm 1n'}} J_{\nu_l}(k_{l \pm 1n'}x) \mp x J'_{\nu_l}(k_{l \pm 1n'}x) \right\} \\ &= \frac{1}{2J'_{\nu_l}(k_{ln})J'_{\nu_{l \pm 1}}(k_{l \pm 1n'})} \left\{ \frac{\nu_l}{k_{l \pm 1n'}} \mp \frac{d}{dk_{l \pm 1n'}} \right\} \int_0^1 dx x J_{\nu_l}(k_{ln}x) J_{\nu_l}(k_{l \pm 1n'}x) \end{aligned}$$

According to Eq. **1.8.3.10**, p. 41 [56], we have

$$\begin{aligned} \int_0^1 dx x J_{\nu_l}(k_{ln}x) J_{\nu_l}(k_{l \pm 1n'}x) &= \frac{k_{ln} J_{\nu_{l+1}}(k_{ln}) J_{\nu_l}(k_{l \pm 1n'}) - k_{l \pm 1n'} J_{\nu_l}(k_{ln}) J_{\nu_{l+1}}(k_{l \pm 1n'})}{k_{l \pm 1n'}^2 - k_{ln}^2} \\ &= k_{ln} \frac{J_{\nu_{l+1}}(k_{ln}) J_{\nu_l}(k_{l \pm 1n'})}{k_{l \pm 1n'}^2 - k_{ln}^2}, \end{aligned}$$

where the simplification in the last equality can be made, because of the definition of the wave numbers  $\{k_{ln}\}_{ln}$  as the  $n^{\text{th}}$  non-zero root of the Bessel function  $J_{\nu_l}$ . Then, after performing some straightforward algebraic manipulations, we arrive at

$$I_{nn'}^{ll \pm 1} = -\frac{k_{ln} k_{l \pm 1n'}}{(k_{l \pm 1n'}^2 - k_{ln}^2)^2}.$$

Finally, putting the previous results together, we obtain the expected matrix elements, for  $l \in \mathbb{N}$ ,  $n \in \mathbb{N}^*$  and  $m \in \llbracket -l, l \rrbracket$ , as

$$\langle \psi_{lnm} | r \cos\theta | \psi_{010} \rangle = 4R I_{n1}^{l0} K_{m0}^{l0} = -\frac{4R}{3} \frac{\pi k_{1n}}{(k_{1n}^2 - \pi^2)^2} \delta_{l1} \delta^{m0}.$$

## References

- [1] N. KIRKSTAEDTER, N. N. LEDENTSOV, M. GRUNDMANN, D. BIMBERG, V. M. USTINOV, S. S. RUVIMOV, M. V. MAXIMOV, P. S. KOPAPOSIEV, Zh. I. ALFEROV, U. RICHTER, P. WERNER, U. GOSELE and J. HEYDENREICH 1994 *Electron. Lett.* **30** 1416.
- [2] T. YOSHIE, A. SCHERER, J. HENDRICKSON, G. KHITROVA, H. M. GIBBS, G. RUPPER, C. ELL, O. B. SHCHEKIN and D. G. DEPPE 2004 *Nature* **432** 200.
- [3] B. TRAUZETTEL, D. V. BULAEV, D. LOSS and G. BURKARD, 2007 *Nature Physics* **3** 192.
- [4] K. ISHIBASHI, M. SUZUKIA, D. TSUYAA and Y. AOYAGIA 2003 *Microelectronic Engineering* **67-68** 749.
- [5] M. K. So, C. Xu, A. M. Loening, S. S. Gambhir and J. Rao 2006 *Nat. Biotechnol.* **24** 339.
- [6] A. I. Ekimov, A. A. Onushchenko and V. A. Tsekhomskii 1980 *Fiz. Khim. Stekla* **6** 511.
- [7] V. V. Golubkov, A. I. Ekimov, A. A. Onushchenko and V. A. Tsekhomskii 1981 *Fiz. Khim. Stekla* **7** 397.
- [8] L. E. Brus 1984 *J. Chem. Phys.* **80** 4403.
- [9] K. Kash, A. Scherer, J. M. Worlock, H. G. Craighead and M. C. Tamargo 1986 *Appl. Phys. Lett.* **49** 1043.
- [10] H. Temkin, G. J. Dolan, M. B. Panish, and S. N. G. Chu 1987 *Appl. Phys. Lett.* **50** 413.
- [11] B. A. Vojak, N. Holonyak, W. D. Laidig, K. Hess, J. J. Coleman and P. D. Dapkus 1980 *Solid State Commun.* **35** 477.
- [12] Al. L. Efros and A. L. Efros 1982 *Soviet Physics. Semicond.* **16** 772.
- [13] L. E. Brus 1983 *J. Chem. Phys.* **79** 5566.
- [14] L. E. Brus 1986 *J. Chem. Phys.* **90** 2555.
- [15] Y. Kayanuma 1988 *Phys. Rev. B* **38** 9797.
- [16] Y. Kayanuma and H. Momiji 1990 *Phys. Rev. B* **41** 10261.
- [17] Y. Kayanuma 1991 *Phys. Rev. B* **44** 13085.
- [18] S. V. Nair, S. Sinha and K. C. Rustagi 1987 *Phys. Rev. B* **35** 4098.
- [19] D. B. Tran Thoai, Y. Z. Hu and S. W. Koch 1990 *Phys. Rev. B* **42** 11261.
- [20] C. F. Lo and R. Sollie 1991 *Solid State Commun.* **79** 775.
- [21] B. G. Potter and J. H. Simmons 1988 *Phys. Rev. B* **37**, 10838
- [22] B. G. Potter and J. H. Simmons 1990 *J. Appl. Phys.* **68** 1218.
- [23] S. Le Goff and B. Stébé 1992 *Solid State Commun.* **83** 555.
- [24] J. W. Brown and H. N. Spector 1987 *Phys. Rev. B* **35** 3009.
- [25] M. H. Degani and O. Hipólito 1987 *Phys. Rev. B* **35** 9345.
- [26] Y. Wang and N. Herron 1990 *Phys. Rev. B* **42** 7253.
- [27] S. Nomura and T. Kobayashi 1991 *Solid State Commun.* **78** 677.
- [28] J.-B. Xia 1989 *Phys. Rev. B* **40** 8500.
- [29] P. C. Sercel and K. J. Vahala 1990 *Phys. Rev. B* **42**, 3690.
- [30] K. J. Vahala and P. C. Sercel 1990 *Phys. Rev. Lett.* **65**, 239.
- [31] A. I. Yakimov, A. V. Dvurechenskii, A. I. Nikiforov, V. V. Ulyanov, A. G. Milekhin, A. O. Govorov, S. Schulze and D. R. T. Zahn 2003 *Phys. Rev. B* **67** 125318.
- [32] V. A. Harutyunyan, K. S. Aramyan and H. Sh. Petrosyan 2004 *Physica E* **21** 53.
- [33] H. Ham and H. Spector 2006 *Physica B* **381** 53 (2006).
- [34] G. Wei, S. Wang and G. Yi 2008 *Microelectron. J.* **39**.

- [35] A. C. Bittencourt, G. E. Marques and C. Trallero-Ginerb 2004 *Solid State Commun.* **129** 57.
- [36] A. H. Rodriguez, L. Meza-Montes, C. Trallero-Giner and S. E. Ulloa 2005 *Phys. Status Solidi B* **242** 1820.
- [37] H.-J. Polland, L. Schultheis, J. Kuhl, E. O. Göbel and C. W. Tu 1985 *Phys. Rev. Lett.* **55** 2610.
- [38] T. H. Wood, C. A. Burrus, D. A. B. Miller, D. S. Chemla, T. C. Damen, A. C. Gossard, and W. Wiegmann 1984 *Appl. Phys. Lett.* **44** 16.
- [39] G. Bastard, E. E. Mendez, L. L. Chang and L. Esaki 1983 *Phys. Rev. B* **28** 3241.
- [40] S. Nomura and T. Kobayashi 1990 *Solid State Commun.* **73** 425.
- [41] S. Nomura and T. Kobayashi 1990 *Solid State Commun.* **74** 1153.
- [42] Y. Chiba and S. Ohnishi 1988 *Phys. Rev. B* **38** 12988.
- [43] A. I. Ekimov, Al. L. Efros, T. V. Shubina and A. P. Skvortsov 1990 *J. Lumin.* **46** 97.
- [44] A. S. Dissanayake, J. Y. Lin, and H. X. Jiang 1995 *Phys. Rev. B* **51** 5457.
- [45] G. W. Wen, J. Y. Lin, H. X. Jiang and Z. Chen 1995 *Phys. Rev. B* **52** 5913.
- [46] K. Chang and J.-B. Xia 1998 *J. Appl. Phys.* **84** 1454.
- [47] O. Keller and T. Garm 1995 *Phys. Rev. B* **52** 4670.
- [48] Y. E. Lozovik and S. Y. Volkov 2003 *Physics of the Solid State* **45** 345.
- [49] P. A. Sundqvist, V. Narayan, J. Vincent and M. Willander 2002 *Physica E* **15** 27.
- [50] J. Pan and M. V. Ramakrishna 1994 *Phys. Rev. B* **50** 15431.
- [51] H. M. Schmidt and H. Weller 1986 *Chem. Phys. Lett.* **129** 615.
- [52] J. J. Hopfield and D. G. Thomas 1963 *Phys. Rev.* **132** 563.
- [53] L. M. Magid 1972 *Electromagnetic Fields, Energy and Waves* (New York: John Wiley & Sons), p.350-370.
- [54] C. Cohen-Tannoudji, B. Diu and F. Laloë 1973 *Mécanique quantique* (Paris: Hermann éditeurs des sciences et des arts), Ch. VI p.689-670.
- [55] A. P. Prudnikov, Yu. A. Brychkov and O. I. Marichev 1998 *Integrals and Series* Vol. 1 *Elementary Functions* (Gordon and Breach Science Publishers).
- [56] A. P. Prudnikov, Yu. A. Brychkov and O. I. Marichev 1998 *Integrals and Series* Vol. 2 *Special Functions* (Gordon and Breach Science Publishers).
- [57] I. S. Gradshteyn and I. M Ryzhik 2000 *Table of Integrals, Series, and Products — Sixth Edition* (San Diego: Academic Press).
- [58] W. Magnus, F. Oberheittinger and R. P. Soni 1966 *Formulas and Theorems for the Special Functions of Mathematical Physics* (New York: Springer).